

Modulational instability of two pairs of counter-propagating waves and energy exchange in two-component media

S.D. Griffiths^a, R.H.J. Grimshaw^b, K.R. Khusnutdinova^b *

^aDepartment of Atmospheric Sciences, University of Washington,
Box 351640, Seattle, WA 98195, USA

^bDepartment of Mathematical Sciences, Loughborough University,
Loughborough, LE11 3TU, UK

Abstract

The dynamics of two pairs of counter-propagating waves in two-component media is considered within the framework of two generally nonintegrable coupled Sine-Gordon equations. We consider the dynamics of weakly nonlinear wave packets, and using an asymptotic multiple-scales expansion we obtain a suite of evolution equations to describe energy exchange between the two components of the system. Depending on the wave packet length-scale *vis-a-vis* the wave amplitude scale, these evolution equations are either four non-dispersive and nonlinearly coupled envelope equations, or four non-locally coupled nonlinear Schrödinger equations. We also consider a set of fully coupled nonlinear Schrödinger equations, even though this system contains small dispersive terms which are strictly beyond the leading order of the asymptotic multiple-scales expansion method. Using both the theoretical predictions following from these asymptotic models and numerical simulations of the original unapproximated equations, we investigate the stability of plane-wave solutions, and show that they may be modulationally unstable. These instabilities can then lead to the formation of localized structures, and to a modification of the energy exchange between the components. When the system is close to being integrable, the time-evolution is distinguished by a remarkable almost periodic sequence of energy exchange scenarios, with spatial patterns alternating between approximately uniform wavetrains and localized structures.

PACS numbers: 02.30 Jr, 02.30 Mv, 46.40 Cd, 47.20 Ky

MSC numbers: 35 Q 55, 41 A 60, 74 J 30, 76 E 30

Keywords: coupled Sine-Gordon equations, amplitude evolution equations, energy exchange in two-component systems, nonlinear Schrödinger equations, modulational instability.

*Corresponding author. Tel.: +44 (0)1509 228202. Fax: +44 (0)1509 223969. E-mail address:
K.Khusnutdinova@lboro.ac.uk

1 Introduction

The dynamics of nonlinear waves is central to understanding the behaviour of a wide range of physical systems. Applications include Langmuir waves in plasmas (e.g. [1]), waves in optical fibres (e.g. [2, 3]), and water waves (e.g. [4] and references therein). An important theme of much of this work has been understanding modulational instabilities of plane waves, and in recent years a particular focus has been the instability of nonlinearly coupled waves. Examples include studies of counter-propagating waves in parametrically forced systems (e.g. [5, 6, 7]), standing water waves (e.g. [8]), co-propagating waves in shallow water [9], and more general energy exchange processes in coupled Sine-Gordon equations [10]. Other interesting recent results related to the dynamics of nonlinearly coupled waves include the rigorous proof of the existence of standing water waves [11], and a study of resonant triad dynamics in weakly damped Faraday waves with two-frequency forcing [12].

Our present study is devoted to multi-component systems that may be modelled by nonlinear partial differential equations with one space dimension x , and with time t , which admit linear stable wave solutions of the form $A \exp i(kx - \omega t)$. Here $\omega = \omega(k)$, where importantly this dispersion relation has several branches. We aim to study the nonlinear development of several plane waves with the same wavenumber k , taking particular care to diagnose any modulational instabilities. As is customary we shall assume that each wave amplitude A is $O(\varepsilon)$ where $\varepsilon \ll 1$, thus enabling the weakly nonlinear regime to be studied using asymptotic methods.

When there is just a single wave, the procedure is well-known. There is a distinguished lengthscale for modulations to the wave amplitude, $O(\varepsilon^{-1})$, on which the effects of dispersion and nonlinearity become simultaneously important, on a timescale $O(\varepsilon^{-2})$. Then, in a reference frame moving with the group velocity of the wave, the governing nonlinear partial differential equations can be reduced via the method of multiple scales to a nonlinear Schrödinger (NLS) equation for the wave amplitude A (e.g. [13]). As is well known, if $\omega''(k)$ has the same sign as the coefficient of the cubic nonlinear term, then a plane wave is modulational unstable [14] (sometimes called a Benjamin–Feir instability, or sideband instability [15]).

One can apply a similar methodology for the case of two waves, possibly counter-propagating, say $A \exp i(kx - \omega_1(k)t) + B \exp i(kx - \omega_2(k)t)$. With the same scaling as above, in general the governing nonlinear partial differential equations can be reduced to non-locally coupled NLS equations for A and B [16, 17, 18]. For unbounded or periodic systems, the coupling terms either disappear or can be eliminated by a phase transformation [17], and so modulational instability is determined by the instability of the individual waves. However, if the group velocities ω'_1 and ω'_2 are equal, or differ only by an $O(\varepsilon)$ quantity, then one obtains locally coupled NLS equations, and there may be additional instabilities solely due to this coupling, even when both waves are individually stable [19, 20].

More generally, one can pursue an asymptotic multiple-scales expansion in which the wave amplitudes, of $O(\varepsilon)$, are modulated on a lengthscale of $O(\sigma^{-1})$. Then, retaining all terms of $O(\varepsilon\sigma, \varepsilon\sigma^2, \varepsilon^3)$, the governing partial differential equations can be reduced to coupled NLS equations for the two wave amplitudes. Expressed here in unscaled variables, they are of the form

$$A_t + v_{g_1} A_x = (i\omega''_1/2)A_{xx} + i\mu_1|A|^2 A + i\mu_2|B|^2 A, \quad (1)$$

where $v_{g_1} = \omega'_1$ is the group velocity, and $\mu_{1,2}$ are constant nonlinear coefficients. There is a corresponding equation for B , with a different transport term due to the group velocity $v_{g_2} = \omega'_2$. On the right-hand side, the linear dispersive terms of $O(\varepsilon\sigma^2)$ are retained, even though these are strictly smaller than the $O(\varepsilon\sigma)$ transport terms on the left-hand side. Note that for a single wave, the transport term can be removed by moving to the group velocity reference frame, but this is generally not possible in coupled systems with differing group velocities. The nonlinear terms on the right-hand side are $O(\varepsilon^3)$, and with the conventional NLS choice that $\sigma = \varepsilon$, these equations can then be systematically reduced to the aforementioned non-locally coupled NLS equations, provided that v_{g_1} is not equal or close to v_{g_2} . Alternatively, one could choose $\sigma = \varepsilon^2$ giving a balance between the transport terms and the nonlinear terms, leading to non-dispersive and nonlinearly coupled envelope equations. Nevertheless, although coupled NLS equations of the form (1) are not generally asymptotically exact, in that they contain small dispersive terms which are strictly beyond the leading order transport

terms, they may be useful as they do capture the leading order dispersive and nonlinear effects. Studies based on this type of approach have recently been made for the parametric generation of waves by an external oscillatory field in the framework of two coupled, damped, parametrically driven NLS equations (see [5, 6, 7] and references therein), and for the interaction of two waves in shallow water in the framework of the KdV equation [9].

The aims of this study are to extend our understanding of the nonlinear behaviour of multiple-wave systems, to derive asymptotic equations to describe many interacting waves, and to assess the applicability and accuracy of the various resulting coupled wave models, with particular reference to the modulational instability of plane waves. This work is performed in the context of energy exchange processes in two-component systems, permitting us to examine explicitly both two-wave and four-wave dynamics. We consider a system of coupled nonlinear Klein–Gordon equations

$$u_{tt} - u_{xx} = f_u(u, w), \quad w_{tt} - c^2 w_{xx} = f_w(u, w), \quad (2)$$

where the subscripts denote partial derivatives. Here, $f(u, w)$ is a potential function for the nonlinear coupling, and c is the ratio of the acoustic velocities of the components u and w . In its simplest form, (2) describes the long-wave dynamics of two coupled one-dimensional periodic chains of particles, the elements of each chain being linked by linear coupling, and the chains themselves being linked by the nonlinear coupling [21]. Applications of this model include nonlinear waves in bi-layers with imperfect interfaces [22, 23], and dynamical processes in DNA [24, 25].

The particular case we shall study is that for which the potential function is $f(u, w) = \cos(\delta u - w) - 1$. Then the system (2) reduces to a set of coupled Sine-Gordon equations:

$$u_{tt} - u_{xx} = -\delta^2 \sin(u - w), \quad w_{tt} - c^2 w_{xx} = \sin(u - w), \quad (3)$$

where the variable u replaces δu , compared to (2). In addition to the two applications mentioned above, the coupled Sine-Gordon equations generalize the Frenkel–Kontorova dislocation model [26] (see also [27], and references therein). As shown in [28], processes involving an exchange of energy between the two components of the system are possible due to the existence of two branches of the dispersion relation. These processes represent a continuum generalization of energy exchange in a system of coupled pendulums [29] (see also [30]). The mechanism of such energy exchange is essentially linear, with energy being transferred between the physical components of the system, rather than the wave components. Therefore, a natural question to ask is, what happens to these linear plane wave solutions under the influence of nonlinearity, especially if they are modulationally perturbed? Here, we are interested in studying such modulational instabilities in a more or less generic situation, in contrast to the recent papers on targeted energy transfer, which placed certain restrictions on the physical properties of the system [31, 32].

First steps in this direction have been made in our recent work [10]. There we dealt with a particular solution of (3) involving only a single pair of waves, and considered its modulational instability in the context of two non-locally coupled NLS equations. In the present study, we generalise this analysis to two pairs of counter-propagating waves, which generally leads to a system of four non-locally coupled NLS equations. Note that the four-wave case is essentially different from the two-wave case, since the number of characteristic variables now differs from the number of independent variables, making the strict derivation of the asymptotic evolution equations not so straightforward. However, as we show here, the same methodology can, in general, be used to derive n non-locally coupled NLS equations for the co-evolution of n waves. We also re-examine the two-wave stability problem using the coupled NLS equations, and compare the predictions with those of the non-locally coupled NLS equations. Throughout, numerical simulations of the governing coupled Sine-Gordon equations are used to assess the various predictions over a range of wave amplitudes.

Our paper is organized as follows. In Section 2, we discuss solutions exhibiting periodic energy exchange between the two components. Section 3 is devoted to the derivation of asymptotic models for weakly nonlinear waves. Specifically, we derive non-locally coupled NLS equations for the regime with modulations on a lengthscale of $O(\varepsilon^{-1})$, and also non-dispersive nonlinearly coupled envelope equations for the regime with modulations on a lengthscale of $O(\varepsilon^{-2})$. Then we motivate the introduction of the coupled NLS equations, and give them for the case of two pairs of counter-propagating

waves (correcting an error in [28]). In Section 4, we study modulational instability of weakly nonlinear coupled two-wave solutions in each of the respective models, extending our previous study [10]. In Section 5, we study modulational instability of weakly nonlinear four-wave solutions, using two asymptotic models. Numerical simulations of the system (3) of coupled Sine-Gordon equations are presented in Section 6, with a focus on the growth of any modulational instabilities, and the numerical results are compared with the theoretical predictions of Sections 4 and 5. We conclude in Section 7.

2 Energy exchange

The system (2) is Lagrangian, with density

$$L = \frac{1}{2}(u_t^2 + w_t^2 - u_x^2 - c^2 w_x^2) + f(u, w).$$

For any function $f(u, w)$, the system (2) has conservation laws for energy and momentum. (In particular cases, there are additional conservation laws, which can be found using results from a Lie group classification of these equations [22], and by using the Noether theorem (e.g. [33])).

The energy conservation law for the system (3) has the form

$$\frac{\partial}{\partial t} \left(\frac{1}{2} (u_t^2 + u_x^2 + \delta^2 w_t^2 + c^2 \delta^2 w_x^2) + \delta^2 (1 - \cos(u - w)) \right) - \frac{\partial}{\partial x} (u_t u_x + c^2 \delta^2 w_t w_x) = 0.$$

For periodic solutions in $0 < x < l$, we define domain integrated average energies

$$E_u = \frac{1}{l} \int_0^l \frac{1}{2} (u_t^2 + u_x^2) dx, \quad E_w = \frac{1}{l} \int_0^l \frac{\delta^2}{2} (w_t^2 + c^2 w_x^2) dx, \quad (4)$$

$$E_c = \frac{1}{l} \int_0^l \delta^2 (1 - \cos(u - w)) dx, \quad (5)$$

describing the energy in the u -component, the energy in the w -component, and the energy of coupling, respectively. Then the domain integrated average energy E is simply

$$E = E_u + E_w + E_c. \quad (6)$$

Although E is constant, we can identify solutions that have a time-periodic exchange of energy between E_u , E_w and E_c .

2.1 Linear solutions

When $|u - w| \ll 1$, the coupled Sine-Gordon equations (3) reduce to a linear system. Looking for a solution of the form $(u, w) = (1, \alpha) \exp i(kx - \omega t) + \text{c.c.}$ leads to the dispersion relation

$$\omega_{1,2}^2 = \frac{1}{2} \left[\nu_1^2 + \nu_2^2 \mp \sqrt{(\nu_1^2 - \nu_2^2)^2 + 4\delta^2} \right], \quad (7)$$

where $\nu_1^2 = \delta^2 + k^2$ and $\nu_2^2 = 1 + c^2 k^2$. The corresponding values of α , giving the ratio w/u , are

$$\alpha_{1,2} = \frac{\nu_1^2 - \omega_{1,2}^2}{\delta^2} = \frac{1}{\nu_2^2 - \omega_{1,2}^2}.$$

We note that $\alpha_1 > 0$, and $\alpha_2 < 0$. For example, if $c = 1$, then $\alpha_1 = 1$ and $\alpha_2 = -\delta^{-2}$.

We first consider a superposition of two linear waves, taken to be right-propagating, with the same positive wavenumber k but different frequencies $\omega_1(k)$ and $\omega_2(k)$. Further, we suppose that one

component, taken to be u , is initially excited, while the other component w is initially at rest. The corresponding initial conditions are

$$\begin{aligned} u(x, 0) &= U \cos kx, & u_t(x, 0) &= \frac{(\omega_1 |\alpha_2| + \omega_2 \alpha_1)}{\alpha_1 + |\alpha_2|} U \sin kx, \\ w(x, 0) &= 0, & w_t(x, 0) &= \frac{(\omega_1 - \omega_2) \alpha_1 |\alpha_2|}{\alpha_1 + |\alpha_2|} U \sin kx, \end{aligned} \quad (8)$$

and one may write the time-dependent solution as

$$u = \tilde{U}(t) \cos(kx - \gamma_+ t - \theta(t)), \quad w = -\frac{2\alpha_1 |\alpha_2|}{\alpha_1 + |\alpha_2|} U \sin \gamma_- t \sin(kx - \gamma_+ t), \quad (9)$$

where

$$\tilde{U}(t) = U \sqrt{1 - \frac{4\alpha_1 |\alpha_2| \sin^2 \gamma_- t}{(\alpha_1 + |\alpha_2|)^2}}, \quad \theta(t) = \arctan \left(\left(\frac{\alpha_1 - |\alpha_2|}{\alpha_1 + |\alpha_2|} \right) \tan \gamma_- t \right), \quad \gamma_{\pm} = \frac{\omega_2 \pm \omega_1}{2}. \quad (10)$$

As discussed in more detail in [10], this solution describes an exchange of energy between waves travelling in the two components u and w . The amplitude of the wave propagating in the u component varies between its initial value U , and a smaller non-zero value $U_{min} = U |\alpha_1 - |\alpha_2|| / (\alpha_1 + |\alpha_2|)$. There is a full exchange in the wave amplitudes from zero to non-zero values when

$$(c^2 - 1)k^2 = \delta^2 - 1. \quad (11)$$

Then $\nu_1^2 = \nu_2^2 = \nu^2$, $\alpha_1 = -\alpha_2 = \delta^{-1}$, and the solution (9) reduces to

$$u = U \cos \gamma_- t \cos(kx - \gamma_+ t), \quad w = -U \delta^{-1} \sin \gamma_- t \sin(kx - \gamma_+ t). \quad (12)$$

This is illustrated in Figure 1, for the case $c = \delta = 1$, $k = 1.6$. If $c = 1$, then (11) can be satisfied only for $\delta = 1$, while k is arbitrary. If $c \neq 1$, then (11) cannot be satisfied if $(\delta^2 - 1)/(c^2 - 1) < 0$. Otherwise, (11) is satisfied for a single wavenumber $k = ((\delta^2 - 1)/(c^2 - 1))^{1/2}$.

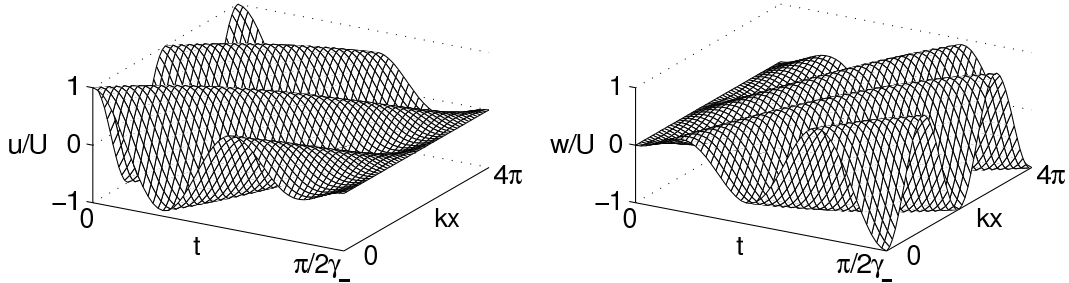


Figure 1: Full exchange in the linear two-wave solution (12).

For the solution (12), the energy is partitioned according to

$$\begin{pmatrix} E_u \\ E_w \\ E_c \end{pmatrix} = \frac{U^2 \cos^2 \gamma_- t}{4} \begin{pmatrix} \gamma_+^2 + k^2 \\ \gamma_-^2 \\ \delta^2 \end{pmatrix} + \frac{U^2 \sin^2 \gamma_- t}{4} \begin{pmatrix} \gamma_+^2 + c^2 k^2 \\ \gamma_-^2 \\ 1 \end{pmatrix}, \quad (13)$$

where, for these linear solutions, E_c is calculated using only the quadratic term of (5). Using $\gamma_-^2 + \gamma_+^2 = \delta^2 + k^2$, one may show from (6) and (13) that $E = U^2 (\delta^2 + k^2) / 2$. From (13) we see that there is a partial exchange of energy between u and w , with period $T = \pi / \gamma_-$. However, if γ_- is small enough, i.e. if the frequencies ω_1 and ω_2 are close enough for some wavenumber k , then at $t = \pi / 2\gamma_-, 3\pi / 2\gamma_-, \dots$

the u -component is almost in equilibrium and almost all of its energy is lost, whilst at $t = 0, \pi/\gamma_-, \dots$ the w -component is almost in equilibrium and almost all of its energy is lost. If $\nu^2 \gg \delta$, then the period T of the energy exchange tends to infinity.

There exists a corresponding solution to (9) consisting of a superposition of two left-propagating waves. A combination of this left-propagating solution and the right-propagating solution (9) is obtained by using the initial conditions

$$u(x, 0) = U \cos kx, \quad u_t(x, 0) = 0, \quad w(x, 0) = 0, \quad w_t(x, 0) = 0. \quad (14)$$

We then obtain a standing wave involving two pairs of counter-propagating waves:

$$u = \tilde{U}(t) \cos(\gamma_+ t + \theta(t)) \cos kx, \quad w = \frac{2\alpha_1 |\alpha_2| U}{\alpha_1 + |\alpha_2|} \sin \gamma_- t \sin \gamma_+ t \cos kx, \quad (15)$$

with $\tilde{U}(t)$, $\theta(t)$ and γ_{\pm} as given by (10). The amplitude of the standing wave in the u component varies between U and U_{\min} , so that once again there is only a partial exchange between the amplitude of the components, unless condition (11) is satisfied. Then, we have a full exchange, and (15) becomes

$$u = U \cos \gamma_- t \cos \gamma_+ t \cos kx, \quad w = U \delta^{-1} \sin \gamma_- t \sin \gamma_+ t \cos kx, \quad (16)$$

where we note that $\gamma_- < \gamma_+$, from (10). This standing wave solution is illustrated in Figure 2, for the case $c = \delta = 1$, $k = 1.6$.

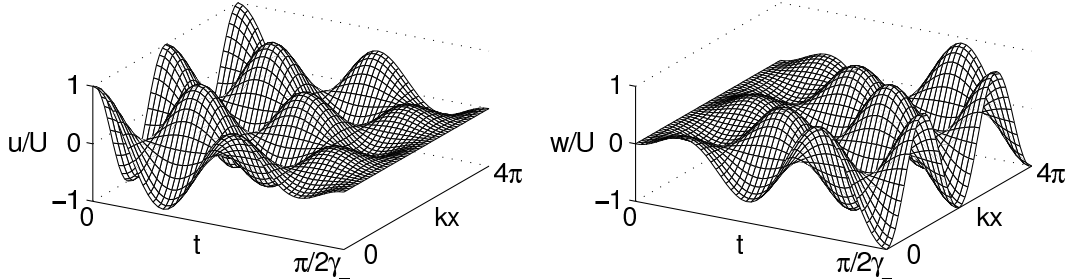


Figure 2: Full exchange in the linear four-wave solution (16).

The energy in solution (16) is $E = U^2(\delta^2 + k^2)/4$, although its partition is rather more complicated than (13). Nevertheless, the general pattern of a partial energy exchange on a timescale π/γ_- remains. For instance, for $\gamma_- \ll 1$ we can say that u loses almost all of its energy near $t = \pi/2\gamma_-, 3\pi/2\gamma_-, \dots$ etc. Some examples of this exchange will be given in the numerical simulations of Section 6.

Note that the role of t and x is interchangeable here; one can consider a superposition of waves with one and the same frequency, but different wavenumbers.

2.2 Nonlinear solutions

An exact nonlinear two-wave solution describing energy exchange between the two components u and w of the system (3) can be found if $c = 1$, i.e., if the characteristic velocities of the components coincide [28]. It is given in terms of Jacobi elliptic functions:

$$\begin{pmatrix} u \\ w \end{pmatrix} = \frac{2}{1 + \delta^2} \left(\arcsin \phi_1 \begin{pmatrix} 1 \\ 1 \end{pmatrix} + \arcsin \phi_2 \begin{pmatrix} \delta^2 \\ -1 \end{pmatrix} \right), \quad \phi_{1,2} = \kappa \operatorname{sn}(kx - \omega_{1,2}(k)t + \theta_0, \kappa), \quad (17)$$

where $\omega_1 = k$, $\omega_2 = \sqrt{1 + \delta^2 + k^2}$, from (7). When $\delta^2 = 1$ (i.e. $\nu_1^2 = \nu_2^2$), the nonlinear solution (17) describes a full periodic exchange between the two components of the system (see [28] for details).

The form of the solution for small amplitude can be calculated by taking the limit $\kappa \rightarrow 0$ in (17). Using the well-known approximation (e.g. [36])

$$\text{sn}(x, \kappa) = \sin x - \frac{1}{4}\kappa^2(x - \sin x \cos x) \cos x + O(\kappa^4),$$

one can eliminate the secular terms by renormalizing the frequencies $\omega_{1,2}(k)$ in the solution (17), and thus find an asymptotic expansion with leading order terms:

$$\begin{pmatrix} u \\ w \end{pmatrix} = \frac{2\kappa}{1 + \delta^2} \left(\sin \left(kx - \omega_1(k)t + \tilde{\theta}_0 \right) \begin{pmatrix} 1 \\ 1 \end{pmatrix} + \sin \left(kx - \omega_2(k)t + \tilde{\theta}_0 + \Omega_2 \kappa^2 t + O(\kappa^4) \right) \begin{pmatrix} \delta^2 \\ -1 \end{pmatrix} \right) + O(\kappa^3), \quad (18)$$

where $\Omega_2 = (1 + \delta^2)/4\omega_2$. Setting $\kappa = U/2$ and $\tilde{\theta}_0 = \pi/2$, the leading order terms of (18) reduce to the linear solution (9) with $c = 1$.

In the general case, when $c \neq 1$, and for a greater number of waves, such exact solutions are not generally available. Instead, we study weakly nonlinear solutions by deriving appropriate asymptotic models. We do this in the next section, and return to these particular energy exchange solutions later.

3 Models for weakly nonlinear wave packets

We consider the weakly nonlinear evolution of pairs of counter-propagating plane waves within system (3). To do this we derive equations for the evolution of wave packets, each with the same dominant wavenumber k . We suppose that the wave amplitudes are characterised by a small parameter $\varepsilon \ll 1$, and thus introduce the asymptotic multiple-scales expansion

$$\begin{pmatrix} u \\ w \end{pmatrix} = \varepsilon \begin{pmatrix} u_1 \\ w_1 \end{pmatrix} + \varepsilon^2 \begin{pmatrix} u_2 \\ w_2 \end{pmatrix} + \varepsilon^3 \begin{pmatrix} u_3 \\ w_3 \end{pmatrix} + O(\varepsilon^4),$$

where

$$\begin{pmatrix} u_1 \\ w_1 \end{pmatrix} = \left[A e^{i(kx - \omega_1 t)} + B e^{i(kx + \omega_1 t)} \right] \begin{pmatrix} 1 \\ \alpha_1 \end{pmatrix} + \left[C e^{i(kx - \omega_2 t)} + D e^{i(kx + \omega_2 t)} \right] \begin{pmatrix} 1 \\ \alpha_2 \end{pmatrix} + \text{c.c.} \quad (19)$$

The coupled Sine-Gordon equations (3) may then be reduced to coupled equations for the slow spatio-temporal evolution of the wave amplitudes A, B, C and D , which are functions of slow variables. We will consider modulations on a long lengthscale χ or on a super-long lengthscale X , with corresponding slow and super-slow timescales τ and T , defined by

$$\chi = \varepsilon x, \quad X = \varepsilon^2 x, \quad \tau = \varepsilon t, \quad T = \varepsilon^2 t. \quad (20)$$

We first derive an asymptotic model for modulations on the super-long lengthscale, leading to a system of four non-dispersive nonlinearly coupled envelope equations. We then do the same for modulations on the long lengthscale, generally leading to a system of four non-locally coupled NLS equations (“averaged equations”). We finally present a third model, the coupled NLS equations, which may be regarded as a model for modulations on the long lengthscale with both the $O(\varepsilon^2)$ transport terms and the $O(\varepsilon^3)$ linear dispersive terms retained.

3.1 The non-dispersive nonlinearly coupled envelope equations

To derive this model, one has to suppose that A, B, C and D are functions of $X = \varepsilon^2 x, T = \varepsilon^2 t$ (see, for example, [34, 35]). At leading order, i.e. $O(\varepsilon)$ in this expansion, we find a linear wave equation for u_1 and w_1 , which is taken to be the four-wave solution (19), with A, B, C and D as yet undetermined

functions of X, T . At the next order, one obtains solvability conditions in the usual way from the equations for u_2 and w_2 , yielding

$$\begin{aligned} A_T + v_{g_1} A_X &= i\mu_1(|A|^2 + 2|B|^2)A + i\mu_2(|C|^2 + |D|^2)A + i\mu_2 B^* C D, \\ B_T - v_{g_1} B_X &= -i\mu_1(|B|^2 + 2|A|^2)B - i\mu_2(|C|^2 + |D|^2)B - i\mu_2 A^* C D, \\ C_T + v_{g_2} C_X &= i\mu_3(|C|^2 + 2|D|^2)C + i\mu_4(|A|^2 + |B|^2)C + i\mu_4 D^* A B, \\ D_T - v_{g_2} D_X &= -i\mu_3(|D|^2 + 2|C|^2)D - i\mu_4(|A|^2 + |B|^2)D - i\mu_4 C^* A B, \end{aligned} \quad (21)$$

where the group velocities v_{g_i} are given by

$$v_{g_i} = \omega'_i = \frac{k}{\omega_i} \frac{1 + \alpha_i^2 \delta^2 c^2}{1 + \alpha_i^2 \delta^2}, \quad (22)$$

and the nonlinear coefficients are

$$\begin{aligned} \mu_1 &= \frac{\delta^2(1 - \alpha_1)^4}{4\omega_1(1 + \alpha_1^2 \delta^2)}, \quad \mu_2 = \frac{\delta^2(1 - \alpha_1)^2(1 - \alpha_2)^2}{2\omega_1(1 + \alpha_1^2 \delta^2)}, \\ \mu_3 &= \frac{\delta^2(1 - \alpha_2)^4}{4\omega_2(1 + \alpha_2^2 \delta^2)}, \quad \mu_4 = \frac{\delta^2(1 - \alpha_1)^2(1 - \alpha_2)^2}{2\omega_2(1 + \alpha_2^2 \delta^2)}. \end{aligned} \quad (23)$$

The equations (21) are non-dispersive.

Note that for the case of two-wave interaction, with $B = D = 0$ for instance, (21) yields the system

$$A_T + v_{g_1} A_X = i(\mu_1|A|^2 + \mu_2|C|^2)A, \quad C_T + v_{g_2} C_X = i(\mu_3|C|^2 + \mu_4|A|^2)C,$$

which is integrable in quadratures [10] (see also [34]).

3.2 The non-locally coupled NLS equations

To derive the second model, we generalise the approach of [16] to the case of four waves. The generalization is not straightforward, since the number of characteristic variables now differs from the number of independent variables, whereas they are the same in the two-wave case. However, these potential difficulties can be readily overcome, and the approach we describe here can generally be applied to any number of waves.

We suppose that A, B, C and D are functions of the long lengthscale $\chi = \varepsilon x$, in which case they must also depend on both slow timescales $\tau = \varepsilon t$ and $T = \varepsilon^2 t$. Once again, at $O(\varepsilon)$ (i.e. the leading order in this expansion), we find a linear wave equation for u_1 and w_1 , which is taken to be the four-wave solution (19), with A, B, C and D as yet undetermined functions of χ, τ and T . At $O(\varepsilon^2)$, there are solvability conditions $A_\tau + v_{g_1} A_\chi = 0$, $B_\tau - v_{g_1} B_\chi = 0$, $C_\tau + v_{g_2} C_\chi = 0$, and $D_\tau - v_{g_2} D_\chi = 0$. Introducing the variables

$$\eta_i = \chi - v_{g_i} \tau, \quad \xi_i = \chi + v_{g_i} \tau, \quad (24)$$

the solvability conditions give

$$A = A(\eta_1, T), \quad B = B(\xi_1, T), \quad C = C(\eta_2, T), \quad D = D(\xi_2, T), \quad (25)$$

i.e. there is a simple functional dependence for each wave amplitude in its own reference frame. If we suppose that our solutions have spatial period l in x , which must satisfy $l \sim \varepsilon^{-1}$ for modulations on the long lengthscale, then A, B, C and D are periodic in η_1, ξ_1, η_2 and ξ_2 respectively, with period $\lambda = \varepsilon l$.

The $O(\varepsilon^2)$ terms in the expansion may then be written as

$$\begin{aligned} \begin{pmatrix} u_2 \\ w_2 \end{pmatrix} &= \left[A_2(\eta_1, \tau, T) e^{i(kx - \omega_1 t)} + B_2(\xi_1, \tau, T) e^{i(kx + \omega_1 t)} \right] \begin{pmatrix} 1 \\ \alpha_1 \end{pmatrix} \\ &\quad + \left[C_2(\eta_2, \tau, T) e^{i(kx - \omega_2 t)} + D_2(\xi_2, \tau, T) e^{i(kx + \omega_2 t)} \right] \begin{pmatrix} 1 \\ \alpha_2 \end{pmatrix} + \text{c.c.} \end{aligned} \quad (26)$$

At $O(\varepsilon^3)$, one obtains solvability conditions in the usual way:

$$\partial_\tau A_2 + A_T = \frac{i}{2} \omega_1'' A_{\eta_1 \eta_1} + i\mu_1 (|A|^2 + 2|B|^2) A + i\mu_2 (|C|^2 + |D|^2) A + i\mu_2 B^* C D, \quad (27)$$

$$\partial_\tau B_2 + B_T = -\frac{i}{2} \omega_1'' B_{\xi_1 \xi_1} - i\mu_1 (|B|^2 + 2|A|^2) B - i\mu_2 (|C|^2 + |D|^2) B - i\mu_2 A^* C D, \quad (28)$$

$$\partial_\tau C_2 + C_T = \frac{i}{2} \omega_2'' C_{\eta_2 \eta_2} + i\mu_3 (|C|^2 + 2|D|^2) C + i\mu_4 (|A|^2 + |B|^2) C + i\mu_4 D^* A B, \quad (29)$$

$$\partial_\tau D_2 + D_T = -\frac{i}{2} \omega_2'' D_{\xi_2 \xi_2} - i\mu_3 (|D|^2 + 2|C|^2) D - i\mu_4 (|A|^2 + |B|^2) D - i\mu_4 C^* A B. \quad (30)$$

Here the partial derivatives of A_2 , B_2 , C_2 and D_2 with respect to τ are evaluated at constant η_1 , ξ_1 , η_2 and ξ_2 respectively, consistent with their functional form (25), the nonlinear coefficients are defined as before in (23), and

$$\omega_i'' = \frac{1 - v_{g_i}^2 + \alpha_i^2 \delta^2 (c^2 - v_{g_i}^2) + 4\omega_i^2 \alpha_i (v_{g_i} - k/\omega_i) (v_{g_i} - c^2 k/\omega_i)}{\omega_i (1 + \alpha_i^2 \delta^2)}. \quad (31)$$

We proceed further by integrating (27) with respect to τ at constant η_1 from 0 to τ_0 , and dividing by τ_0 . Letting $\tau_0 \rightarrow \infty$, and demanding that A_2 remains bounded in this limit, yields

$$\begin{aligned} A_T = \frac{i}{2} \omega_1'' A_{\eta_1 \eta_1} + i\mu_1 |A|^2 A + iA \lim_{\tau_0 \rightarrow \infty} \left(\frac{1}{\tau_0} \int_0^{\tau_0} (2\mu_1 |B|^2 + \mu_2 |C|^2 + \mu_2 |D|^2) d\tau \right) \\ + i\mu_2 \lim_{\tau_0 \rightarrow \infty} \left(\frac{1}{\tau_0} \int_0^{\tau_0} B^* C D d\tau \right), \end{aligned}$$

where we have recalled that $A = A(\eta_1, T)$, and where the integrals are taken at constant η_1 . Noting the functional forms (25), we may use (24) to convert the terms involving $|B|^2$, $|C|^2$ and $|D|^2$ into integrals with respect to ξ_1 , η_2 and ξ_2 respectively, still at fixed η_1 , eventually yielding

$$\begin{aligned} A_T = \frac{i}{2} \omega_1'' A_{\eta_1 \eta_1} + i\mu_1 |A|^2 A + i\mu_2 \lim_{\tau_0 \rightarrow \infty} \left(\frac{1}{\tau_0} \int_0^{\tau_0} B^* C D d\tau \right) \\ + iA \lim_{\tau_0 \rightarrow \infty} \frac{1}{\tau_0} \left(2\mu_1 \int_{\eta_1}^{\eta_1 + \tau_0} |B|^2 d\xi_1 + \mu_2 \int_{\eta_1}^{\eta_1 + \tau_0} |C|^2 d\eta_2 + \mu_2 \int_{\eta_1}^{\eta_1 + \tau_0} |D|^2 d\xi_2 \right). \quad (32) \end{aligned}$$

Here τ_0 has been rescaled in each of the final three integrals, and to perform this rescaling we have assumed that v_{g_1} and v_{g_2} are both $O(1)$, with $(v_{g_1} - v_{g_2}) = O(1)$. Finally, we use the periodicity of B , C and D to convert the final three integral terms of (32) to averages over one period. Performing similar operations for (28), (29) and (30) gives

$$\begin{aligned} A_T &= \frac{i}{2} \omega_1'' A_{\eta_1 \eta_1} + i\mu_1 \left(|A|^2 + 2\overline{|B|^2} \right) A + i\mu_2 \left(\overline{|C|^2} + \overline{|D|^2} \right) A + i\mu_2 \lim_{\tau_0 \rightarrow \infty} \left(\frac{1}{\tau_0} \int_0^{\tau_0} B^* C D d\tau \right), \\ B_T &= -\frac{i}{2} \omega_1'' B_{\xi_1 \xi_1} - i\mu_1 \left(2\overline{|A|^2} + \overline{|B|^2} \right) B - i\mu_2 \left(\overline{|C|^2} + \overline{|D|^2} \right) B - i\mu_2 \lim_{\tau_0 \rightarrow \infty} \left(\frac{1}{\tau_0} \int_0^{\tau_0} A^* C D d\tau \right), \\ C_T &= \frac{i}{2} \omega_2'' C_{\eta_2 \eta_2} + i\mu_3 \left(|C|^2 + 2\overline{|D|^2} \right) C + i\mu_4 \left(\overline{|A|^2} + \overline{|B|^2} \right) C + i\mu_4 \lim_{\tau_0 \rightarrow \infty} \left(\frac{1}{\tau_0} \int_0^{\tau_0} D^* A B d\tau \right), \\ D_T &= -\frac{i}{2} \omega_2'' D_{\xi_2 \xi_2} - i\mu_3 \left(2\overline{|C|^2} + \overline{|D|^2} \right) D - i\mu_4 \left(\overline{|A|^2} + \overline{|B|^2} \right) D - i\mu_4 \lim_{\tau_0 \rightarrow \infty} \left(\frac{1}{\tau_0} \int_0^{\tau_0} C^* A B d\tau \right), \end{aligned} \quad (33)$$

where

$$\begin{aligned} \overline{|A|^2}(T) &= \frac{1}{\lambda} \int_0^\lambda |A|^2 d\eta_1, & \overline{|B|^2}(T) &= \frac{1}{\lambda} \int_0^\lambda |B|^2 d\xi_1, \\ \overline{|C|^2}(T) &= \frac{1}{\lambda} \int_0^\lambda |C|^2 d\eta_2, & \overline{|D|^2}(T) &= \frac{1}{\lambda} \int_0^\lambda |D|^2 d\xi_2. \end{aligned}$$

These non-locally coupled NLS equations govern the weakly nonlinear evolution of the wave amplitudes in the general case, when v_{g1} , v_{g2} and $(v_{g1} - v_{g2})$ are all $O(1)$.

If v_{g1} , v_{g2} are $O(1)$ but $(v_{g1} - v_{g2}) = O(\varepsilon)$, then the averaging process described above fails, and we write

$$v_{g1} = \bar{v}_g - \varepsilon\Delta, \quad v_{g2} = \bar{v}_g + \varepsilon\Delta, \quad \text{where } \bar{v}_g = \frac{v_{g1} + v_{g2}}{2}, \quad \Delta = \frac{v_{g2} - v_{g1}}{2\varepsilon}. \quad (34)$$

Then, rather than (25), the solvability conditions at $O(\varepsilon)$ give $A = A(\bar{\eta}, T)$, $B = B(\bar{\xi}, T)$, $C = C(\bar{\eta}, T)$, $D = D(\bar{\xi}, T)$, where

$$\bar{\eta} = \chi - \bar{v}_g\tau, \quad \bar{\xi} = \chi + \bar{v}_g\tau.$$

At $O(\varepsilon^3)$ we obtain equations similar to (27)–(30), but with additional terms $-\Delta A_\chi$, ΔB_χ , ΔC_χ , $-\Delta D_\chi$ on the left-hand side. We then once again perform an averaging operation, yet this time A and C are now both functions of $\bar{\eta}$ and T , whilst B and D are both functions of $\bar{\xi}$ and T . Thus, the final integral terms can be considerably simplified, and rather than (33) we obtain

$$\begin{aligned} A_T - \Delta A_{\bar{\eta}} &= \frac{i}{2} \omega_1'' A_{\bar{\eta}\bar{\eta}} + i\mu_1 \left(|A|^2 + 2\overline{|B|^2} \right) A + i\mu_2 \left(|C|^2 + \overline{|D|^2} \right) A + i\mu_2 \overline{B^* D} C, \\ B_T + \Delta B_{\bar{\xi}} &= -\frac{i}{2} \omega_1'' B_{\bar{\xi}\bar{\xi}} - i\mu_1 \left(2\overline{|A|^2} + |B|^2 \right) B - i\mu_2 \left(\overline{|C|^2} + |D|^2 \right) B - i\mu_2 \overline{A^* C} D, \\ C_T + \Delta C_{\bar{\eta}} &= \frac{i}{2} \omega_2'' C_{\bar{\eta}\bar{\eta}} + i\mu_3 \left(|C|^2 + 2\overline{|D|^2} \right) C + i\mu_4 \left(|A|^2 + \overline{|B|^2} \right) C + i\mu_4 \overline{D^* B} A, \\ D_T - \Delta D_{\bar{\xi}} &= -\frac{i}{2} \omega_2'' D_{\bar{\xi}\bar{\xi}} - i\mu_3 \left(2\overline{|C|^2} + |D|^2 \right) D - i\mu_4 \left(\overline{|A|^2} + |B|^2 \right) D - i\mu_4 \overline{C^* A} B, \end{aligned} \quad (35)$$

with the coefficients defined as before. There is now a local coupling between the A and C modes, and between the B and D modes.

If one permits v_{g1} and v_{g2} to be $O(\varepsilon)$, then three other scenarios arise in which the averaging process fails. If $v_{g1} = O(\varepsilon)$ but $v_{g2} = O(1)$, then using the obvious extension of the above analysis one obtains a system in which A and B are locally coupled, whilst C and D satisfy non-locally coupled NLS equations. If $v_{g2} = O(\varepsilon)$ but $v_{g1} = O(1)$, then C and D are locally coupled, whilst A and B satisfy non-locally coupled NLS equations. If both v_{g1} and v_{g2} are both $O(\varepsilon)$, then something slightly different occurs. Rather than (25), the solvability conditions at $O(\varepsilon)$ give $A = A(\chi, T)$, $B = B(\chi, T)$, $C = C(\chi, T)$, $D = D(\chi, T)$. At $O(\varepsilon^3)$, the averaging operation immediately yields a system of coupled NLS equation for A , B , C and D , with no non-local coupling, which is equivalent to system (36) introduced below. However, none of these scenarios are further considered here, since v_{g1} and v_{g2} are typically $O(1)$ for the Sine-Gordon system (3).

3.3 The coupled NLS equations

An alternative approach is to seek a system with linear dispersive terms, unlike (21), only local nonlinear coupling, unlike (33) and (35), and with no a priori restrictions on the size of the group velocities, unlike (33), (35) and the other systems mentioned at the end of Section 3.2. Such a model is obtained, for instance, by allowing the wave amplitudes A , B , C and D to depend on the long lengthscale $\chi = \varepsilon x$ and the slow timescale $\tau = \varepsilon t$, whilst retaining all terms up to order $O(\varepsilon^3)$. The result is

$$\begin{aligned} A_\tau + v_{g1} A_\chi - \frac{i}{2} \varepsilon \omega_1'' A_{\chi\chi} &= i\mu_1 \varepsilon (|A|^2 + 2|B|^2) A + i\mu_2 \varepsilon (|C|^2 + |D|^2) A + i\mu_2 \varepsilon B^* C D, \\ B_\tau - v_{g1} B_\chi + \frac{i}{2} \varepsilon \omega_1'' B_{\chi\chi} &= -i\mu_1 \varepsilon (2|A|^2 + |B|^2) B - i\mu_2 \varepsilon (|C|^2 + |D|^2) B - i\mu_2 \varepsilon A^* C D, \\ C_\tau + v_{g2} C_\chi - \frac{i}{2} \varepsilon \omega_2'' C_{\chi\chi} &= i\mu_3 \varepsilon (|C|^2 + 2|D|^2) C + i\mu_4 \varepsilon (|A|^2 + |B|^2) C + i\mu_4 \varepsilon D^* A B, \\ D_\tau - v_{g2} D_\chi + \frac{i}{2} \varepsilon \omega_2'' D_{\chi\chi} &= -i\mu_3 \varepsilon (2|C|^2 + |D|^2) D - i\mu_4 \varepsilon (|A|^2 + |B|^2) D - i\mu_4 \varepsilon C^* A B. \end{aligned} \quad (36)$$

In this form the linear dispersive and nonlinear terms are of the same relative order, but $O(\varepsilon)$ smaller than the transport terms. If instead we had used the variables $X = \varepsilon^2 x$, $T = \varepsilon^2 t$, then we would have had a balance between the transport terms and the nonlinear terms, with the linear dispersive terms being relatively $O(\varepsilon^2)$. Only in certain special cases may one simply rescale x and t so that all terms of (36) are simultaneously of the same order. For instance, if only one wave is present, then in a reference frame moving at the group velocity of the wave one may use $T = \varepsilon^2 t$ and $\chi = \varepsilon x$. Similarly, if $B = D = 0$, and $v_{g1} = v_{g2}$, one may perform the same operation to obtain coupled NLS equations for A and C .

Nevertheless, (36) is an appealing model on purely physical grounds. Higher order terms, both linear and nonlinear, could, in principle, be dynamically important. Indeed, since the effects of transport, dispersion, and leading order nonlinearity are captured, models of this type are widely used in studies of weakly nonlinear wave phenomena, as mentioned already in the Introduction. There is an analogy here with the well-known Boussinesq equations often used to model the two-way propagation of water waves. Indeed, any of the asymptotic models (21), (33) and (35) already introduced, or those mentioned at the end of Section 3.2, can be derived from (36) by an asymptotic multiple-scales reduction on the appropriate length and time-scales.

Note that one can deduce (36) without recourse to a new asymptotic expansion. With the usual approach (e.g. [37, 38]), the terms on the left-hand side of (36) result from a Taylor series expansion of the dispersion relation about the dominant wavenumber of that packet. Only the first two terms are retained. The terms on the right-hand side are the relevant nonlinear terms, as already obtained in (21), for instance.

4 Modulational instability of two-wave solutions

It is well known that dispersive weakly nonlinear systems of the type being studied can support modulational instabilities. Some simple examples of this for two-wave solutions were given in our previous study [10]. These results are briefly summarised in Section 4.2. Then, in Sections 4.3 and 4.4, the analysis is extended to the other asymptotic models derived in Section 3.

4.1 Plane waves

We consider the modulational instability of spatially uniform coupled plane wave solutions of the form

$$A = A_0 e^{i\Omega_a T}, \quad C = C_0 e^{i\Omega_c T}, \quad B_0 = D_0 = 0. \quad (37)$$

This is a solution of the non-dispersive nonlinearly coupled envelope (21) model, the non-locally coupled NLS models (33) and (35), and the coupled NLS model (36), provided

$$\Omega_a = \mu_1 |A_0|^2 + \mu_2 |C_0|^2, \quad \Omega_c = \mu_3 |C_0|^2 + \mu_4 |A_0|^2.$$

Substituting (37) into (19) we obtain the leading order solution in the form of two counter-propagating waves:

$$\begin{pmatrix} u \\ w \end{pmatrix} = \varepsilon A_0 e^{i(kx - (\omega_1 - \varepsilon^2 \Omega_a) t)} \begin{pmatrix} 1 \\ \alpha_1 \end{pmatrix} + \varepsilon C_0 e^{i(kx - (\omega_2 - \varepsilon^2 \Omega_c) t)} \begin{pmatrix} 1 \\ \alpha_2 \end{pmatrix} + \text{c.c.} + O(\varepsilon^2). \quad (38)$$

This solution describes a weakly nonlinear interaction between the two components. For $\varepsilon \neq 0$, it generalises the linear energy exchange solutions of Section 2.1 by nonlinearity-induced corrections of $O(\varepsilon^2)$ to the frequencies $\omega_{1,2}(k)$ of the linear waves, given by (7). For $\varepsilon \rightarrow 0$, it reduces to the two-wave linear solution (9) if

$$\varepsilon A_0 = \frac{|\alpha_2| U}{2(\alpha_1 + |\alpha_2|)}, \quad \varepsilon C_0 = \frac{\alpha_1 U}{2(\alpha_1 + |\alpha_2|)}. \quad (39)$$

In the case $c = 1$, (38) matches the weakly nonlinear expansion (18) of the exact two-wave energy-exchange solution (17). Since $\alpha_1 = 1$ and $\alpha_2 = -\delta^{-2}$ at $c = 1$, from (23) $\mu_1 = \mu_2 = \mu_4 = 0$, and

$\mu_3 = (1 + \delta^2)^3 / (4\omega_2 \delta^4)$, so that taking

$$\varepsilon A_0 = \frac{\kappa}{1 + \delta^2}, \quad \varepsilon C_0 = \frac{\kappa \delta^2}{1 + \delta^2}, \quad B_0 = D_0 = 0,$$

we find $\Omega_a = 0$, $\varepsilon^2 \Omega_c = \mu_3 |\varepsilon C_0|^2 = \kappa^2 (1 + \delta^2) / 4\omega_2$, in agreement with (18).

4.2 Previous results

In [10] we considered the stability of the coupled plane wave solutions (37) in the context of two of the asymptotic models of Section 3. Firstly, we showed that the non-dispersive nonlinearly coupled envelope equations (21) with $B = D = 0$ do not support any modulational instabilities. Secondly, we studied instabilities with modulations on the long lengthscale $\chi = \varepsilon x$, with $v_{g1} - v_{g2}$ non-zero and $O(1)$, so that we used (33) with $B = D = 0$. However, the dynamics of that system are relatively simple, since as in [17] the equations may be transformed to two uncoupled NLS equations using the nonlocal transformation

$$\begin{aligned} A(\eta_1, T) &= \tilde{A}(\eta_1, T) \exp \left(i\mu_2 \int_0^T \overline{|C|^2}(T') dT' \right), \\ C(\eta_2, T) &= \tilde{C}(\eta_2, T) \exp \left(i\mu_4 \int_0^T \overline{|A|^2}(T') dT' \right). \end{aligned} \quad (40)$$

Alternatively, stability results can be established directly by looking for solutions of (33) of the form

$$\begin{aligned} A(\eta_1, T) &= A_0(T) \left(1 + a_1 e^{i(\hat{\kappa}\eta_1 - \hat{\Omega}_a T)} + a_2^* e^{-i(\hat{\kappa}\eta_1 - \hat{\Omega}_a^* T)} \right), \\ C(\eta_2, T) &= C_0(T) \left(1 + c_1 e^{i(\hat{\kappa}\eta_2 - \hat{\Omega}_c T)} + c_2^* e^{-i(\hat{\kappa}\eta_2 - \hat{\Omega}_c^* T)} \right), \end{aligned} \quad (41)$$

representing sinusoidal perturbations to the coupled-wave solution (37). Neglecting terms quadratic in disturbance amplitude, (33) leads to two uncoupled linear systems, as expected from (40), with corresponding dispersion relations

$$\hat{\Omega}_a^2 = -\mu_1 |A_0|^2 \omega_1'' \hat{k}^2 + \frac{\omega_1''^2 \hat{k}^4}{4}, \quad \hat{\Omega}_c^2 = -\mu_3 |C_0|^2 \omega_2'' \hat{k}^2 + \frac{\omega_2''^2 \hat{k}^4}{4}. \quad (42)$$

Using (20) and (24) we can rewrite these in terms of an unscaled disturbance wavenumber \hat{k} and frequency $\hat{\omega}$, via

$$\varepsilon \hat{\kappa} = \hat{k}, \quad \varepsilon^2 \hat{\Omega}_a = \hat{\omega}_a - \hat{k} v_{g1}, \quad \varepsilon^2 \hat{\Omega}_c = \hat{\omega}_c - \hat{k} v_{g2}, \quad (43)$$

giving

$$\left(\hat{\omega}_a - \hat{k} v_{g1} \right)^2 = -\mu_1 |\varepsilon A_0|^2 \omega_1'' \hat{k}^2 + \frac{\omega_1''^2 \hat{k}^4}{4}, \quad \left(\hat{\omega}_c - \hat{k} v_{g2} \right)^2 = -\mu_3 |\varepsilon C_0|^2 \omega_2'' \hat{k}^2 + \frac{\omega_2''^2 \hat{k}^4}{4}, \quad (44)$$

where for formal validity we need $A_0, C_0 = O(1)$, $\hat{k} = O(\varepsilon)$, and $(v_{g1} - v_{g2}) = O(1)$.

From (23), we see that $\mu_1 > 0$ and $\mu_3 > 0$, so there will be instability only if $\omega_1'' > 0$ or $\omega_2'' > 0$. Using (31), we can show that ω_2'' is always positive. Thus for sufficiently small \hat{k} there will be a root for $\hat{\omega}_c$ with positive imaginary part, corresponding to an unstable mode. Using (7), we can show that $\omega_1'' < 0$ for small k , whilst $\omega_1'' > 0$ for large k , tending to zero at infinity. Thus $\hat{\omega}_a$ is real for small k , and hence does not correspond to an unstable mode, whilst for larger k , where $\omega_1'' > 0$, it will correspond to an unstable mode for sufficiently small \hat{k} .

4.3 New results: the coupled NLS equations

We now consider instability in the context of the two other asymptotic models of Section 3. The first model is for modulations on the long lengthscale $\chi = \varepsilon x$, but with $(v_{g1} - v_{g2}) = O(\varepsilon)$. Then we must use equations (35), with $B = D = 0$, giving a system that is locally coupled in A and C . The second model is the coupled NLS equations (36), with $B = D = 0$. However, with the appropriate rescaling, it is easy to see that these two systems of equations are equivalent. Therefore, even though the two models were derived in different ways, they may be analysed together.

We look for disturbances to the coupled-wave solution (37) in the form

$$A = A_0(T) \left(1 + a_1 e^{i(\hat{k}x - \hat{\omega}_{ac}t)} + a_2^* e^{-i(\hat{k}x - \hat{\omega}_{ac}^*t)} \right),$$

$$C = C_0(T) \left(1 + c_1 e^{i(\hat{k}x - \hat{\omega}_{ac}t)} + c_2^* e^{-i(\hat{k}x - \hat{\omega}_{ac}^*t)} \right),$$

where we find it convenient to revert to the original unscaled variables x, t and work in terms of the unscaled disturbance frequency $\hat{\omega}$ and wavenumber \hat{k} . Substituting into (35) or (36) we obtain:

$$\begin{aligned} \left(\hat{\omega}_{ac} - \hat{k}v_{g1} - \frac{1}{2}\omega_1''\hat{k}^2 + \mu_1|\varepsilon A_0|^2 \right) a_1 + \mu_1|\varepsilon A_0|^2 a_2 + \mu_2|\varepsilon C_0|^2 c_1 + \mu_2|\varepsilon C_0|^2 c_2 &= 0, \\ -\mu_1|\varepsilon A_0|^2 a_1 + \left(\hat{\omega}_{ac} - \hat{k}v_{g1} + \frac{1}{2}\omega_1''\hat{k}^2 - \mu_1|\varepsilon A_0|^2 \right) a_2 - \mu_2|\varepsilon C_0|^2 c_1 - \mu_2|\varepsilon C_0|^2 c_2 &= 0, \\ \mu_4|\varepsilon A_0|^2 a_1 + \mu_4|\varepsilon A_0|^2 a_2 + \left(\hat{\omega}_{ac} - \hat{k}v_{g2} - \frac{1}{2}\omega_2''\hat{k}^2 + \mu_3|\varepsilon C_0|^2 \right) c_1 + \mu_3|\varepsilon C_0|^2 c_2 &= 0, \\ -\mu_4|\varepsilon A_0|^2 a_1 - \mu_4|\varepsilon A_0|^2 a_2 - \mu_3|\varepsilon C_0|^2 c_1 + \left(\hat{\omega}_{ac} - \hat{k}v_{g2} + \frac{1}{2}\omega_2''\hat{k}^2 - \mu_3|\varepsilon C_0|^2 \right) c_2 &= 0. \end{aligned}$$

This four-by-four linear homogeneous system of equations must have a vanishing determinant, from which we find that

$$Q_a(\hat{v}, \hat{k})Q_c(\hat{v}, \hat{k}) = R, \quad \text{where } R = \mu_2\mu_4\omega_1''\omega_2''|\varepsilon A_0|^2|\varepsilon C_0|^2, \quad (45)$$

$$Q_a(\hat{v}, \hat{k}) = (\hat{v} - v_{g1})^2 - \frac{\omega_1''\hat{k}^2}{4} + \mu_1\omega_1''|\varepsilon A_0|^2, \quad Q_c(\hat{v}, \hat{k}) = (\hat{v} - v_{g2})^2 - \frac{\omega_2''\hat{k}^2}{4} + \mu_3\omega_2''|\varepsilon C_0|^2. \quad (46)$$

Here $\hat{v} = \hat{\omega}_{ac}/\hat{k}$ is the phase speed of the disturbance, whilst R is proportional to the coupling constants in (35) and (36). Note that $Q_a = 0$ and $Q_c = 0$ are the dispersion relations for the uncoupled NLS equations for A and C respectively, cf. (44). Equation (45) is a fourth-order dispersion relation with real coefficients for \hat{v} . Complex solutions for \hat{v} imply modulational instability.

4.4 Instability analysis: the coupled NLS equations

Working within the context of (35), for formal validity of (45) we need $A_0, C_0 = O(1)$, $\hat{k} = O(\varepsilon)$, and $(v_{g1} - v_{g2}) = O(\varepsilon)$. However, within the context of (36), there are no specific scale restrictions, and we may investigate different scaling regimes.

We first probe the effects of the dispersive terms for modulations on the super-long lengthscale, by taking $\hat{k} = \varepsilon^2 \hat{K}$, with $\hat{K} = O(1)$ and $\varepsilon \ll 1$. Writing $\hat{v} = \hat{v}_1 + \varepsilon^2 \hat{v}_2 + \dots$, one may derive expressions for the four roots as

$$(\hat{v} - v_{g1})^2 = -\varepsilon^2 \mu_1 \omega_1'' |A_0|^2 + \varepsilon^4 \left(\frac{1}{4} \omega_1''^2 \hat{K}^2 + \frac{\mu_2 \mu_4 \omega_1'' \omega_2'' |A_0|^2 |C_0|^2}{(v_{g1} - v_{g2})^2} \right) + O(\varepsilon^6),$$

$$(\hat{v} - v_{g2})^2 = -\varepsilon^2 \mu_3 \omega_2'' |C_0|^2 + \varepsilon^4 \left(\frac{1}{4} \omega_2''^2 \hat{K}^2 + \frac{\mu_2 \mu_4 \omega_1'' \omega_2'' |A_0|^2 |C_0|^2}{(v_{g1} - v_{g2})^2} \right) + O(\varepsilon^6).$$

Since $\mu_3 > 0$ and $\omega_2'' > 0$, at least one pair of roots for \hat{v} is complex, and hence there is always an unstable mode. Since $\mu_1 > 0$, there will be an additional unstable mode if $\omega_1'' > 0$. Thus, our analysis suggests that the dispersive terms are destabilising for disturbances on the super-long lengthscale, leading to an instability with a growth rate of $O(\varepsilon^3)$. This is consistent with the nondispersive analysis of [10], mentioned in Section 4.2, which showed there will be no instabilities on the super-long lengthscale with growth rates of $O(\varepsilon^2)$.

We can recover results for modulations on the long lengthscale by taking $\hat{k} = \varepsilon \hat{\kappa}$, with $\hat{\kappa} = O(1)$ and $\varepsilon \ll 1$. If $(v_{g1} - v_{g2}) = O(1)$, then writing $\hat{v} = \hat{v}_1 + \varepsilon \hat{v}_2 + \dots$, one may derive expressions for the four roots as

$$\begin{aligned} (\hat{v} - v_{g1})^2 &= -\varepsilon^2 \left(\mu_1 \omega_1'' |A_0|^2 - \frac{1}{4} \omega_1''^2 \hat{\kappa}^2 \right) + \frac{\varepsilon^4 \mu_2 \mu_4 \omega_1'' \omega_2'' |A_0|^2 |C_0|^2}{(v_{g1} - v_{g2})^2} + O(\varepsilon^6), \\ (\hat{v} - v_{g2})^2 &= -\varepsilon^2 \left(\mu_3 \omega_2'' |C_0|^2 - \frac{1}{4} \omega_2''^2 \hat{\kappa}^2 \right) + \frac{\varepsilon^4 \mu_2 \mu_4 \omega_1'' \omega_2'' |A_0|^2 |C_0|^2}{(v_{g1} - v_{g2})^2} + O(\varepsilon^6). \end{aligned} \quad (47)$$

Since $\mu_3 > 0$ and $\omega_2'' > 0$, there will be an instability with a growth rate of $O(\varepsilon^2)$ if $\hat{\kappa}^2 < 4\mu_3 |C_0|^2 / \omega_2''$. Since $\mu_1 > 0$, there will be an additional unstable mode if $\omega_1'' > 0$ and $\hat{\kappa}^2 < 4\mu_1 |A_0|^2 / \omega_1''$. This is consistent with (42) and (44), derived formally from the non-locally coupled NLS equations. If $(v_{g1} - v_{g2}) = O(\varepsilon)$, then no further approximation of (45) is possible, since it is already the asymptotically consistent model for this regime.

More generally, we now consider the properties of the roots $\hat{v}(\hat{k})$ of (45) without any scale restrictions on \hat{k} or ε . First, if $\hat{k} \gg 1$, then the roots of (45) are approximately $\hat{v} = \pm \omega_1'' \hat{k} / 2$ and $\hat{v} = \pm \omega_2'' \hat{k} / 2$, so that there is stability. We then consider how the roots vary as \hat{k} is reduced from infinity, with all other parameters fixed. Note that these other parameters consist of the plane wave parameters k , $|\varepsilon A_0|$ and $|\varepsilon C_0|$, and the system parameters c and δ . We consider the graph of $Q = Q_a(\hat{v}, \hat{k})Q_c(\hat{v}, \hat{k})$ as a fourth order polynomial in \hat{v} , as \hat{k} is varied. Stability occurs whenever this graph intersects the line $Q = R$ four times, and otherwise there is instability. Note that R is independent of \hat{k} and so this line is immovable as \hat{k} is varied. Noting that μ_2, μ_4 and ω_2'' are all positive, R takes the same sign as ω_1'' . There are thus two possible cases to consider:

1. Suppose first that $\omega_1'' < 0$, so that $R < 0$. For sufficiently large \hat{k} , both uncoupled modes are stable and so $Q_a Q_c$ has four real zeros, $\hat{v}_i, i = 1, 2, 3, 4$ where $\hat{v}_1 > \hat{v}_2, \hat{v}_3 > \hat{v}_4$ are the zeros of Q_a, Q_c respectively. Since $\mu_1 > 0$ and $\omega_1'' < 0$ here, $\hat{v}_{1,2}$ are real for all \hat{k} , from (46). But as \hat{k} is reduced from infinity, there is a critical value of $\hat{k} = \hat{k}_{c2} = 2|\varepsilon C_0|(\mu_3 / \omega_2'')^{1/2}$, at which $\hat{v}_3 = \hat{v}_4 = v_{g2}$, and below which $\hat{v}_{3,4}$ become complex, so that the uncoupled C -mode is then unstable. The issue then is whether the coupling in (45) suppresses or enhances this instability. Consider then the situation when $\hat{k} = \hat{k}_{c2}$, so that $Q_c = (\hat{v} - v_{g2})^2$ and $Q_a = (\hat{v} - v_{g1})^2 - \beta^2$, where

$$\beta^2 = (\omega_1'' / \omega_2'') (\mu_3 \omega_1'' |\varepsilon C_0|^2 - \mu_1 \omega_2'' |\varepsilon A_0|^2) > 0. \quad (48)$$

There are two sub-cases to consider:

- (a) If $|v_{g2} - v_{g1}| \geq \beta$, then the double zero v_{g2} of $Q_c(\hat{v}, \hat{k}_{c2})$ does not lie in (\hat{v}_2, \hat{v}_1) . This scenario is depicted in Figure 3a. Since $R < 0$, $Q_a(\hat{v}, \hat{k}_{c2})Q_c(\hat{v}, \hat{k}_{c2}) = R$ must have at least two complex roots, so that the coupled system is unstable at $\hat{k} = \hat{k}_{c2}$, and therefore for some $\hat{k} > \hat{k}_{c2}$. In this sense we can say that coupling is destabilizing. Indeed, in this case the system remains unstable for all $\hat{k} < \hat{k}_c$, where $\hat{k}_c > \hat{k}_{c2}$ is the critical value at which the system first becomes unstable, and is the value of \hat{k} at which the line $Q = R$ is tangent to the graph of $Q = Q_a Q_c$.
- (b) If $|v_{g2} - v_{g1}| < \beta$, then the double zero v_{g2} of $Q_c(\hat{v}, \hat{k}_{c2})$ lies in (\hat{v}_2, \hat{v}_1) . This scenario is depicted in Figure 3b. Stability at $\hat{k} = \hat{k}_{c2}$ is then determined by

$$R_c = \max(Q_a(\hat{v}_\pm, \hat{k}_{c2})Q_c(\hat{v}_\pm, \hat{k}_{c2})), \quad \hat{v}_\pm = v_{g2} + \frac{3(v_{g1} - v_{g2}) \pm \sqrt{(v_{g1} - v_{g2})^2 + 8\beta^2}}{4},$$

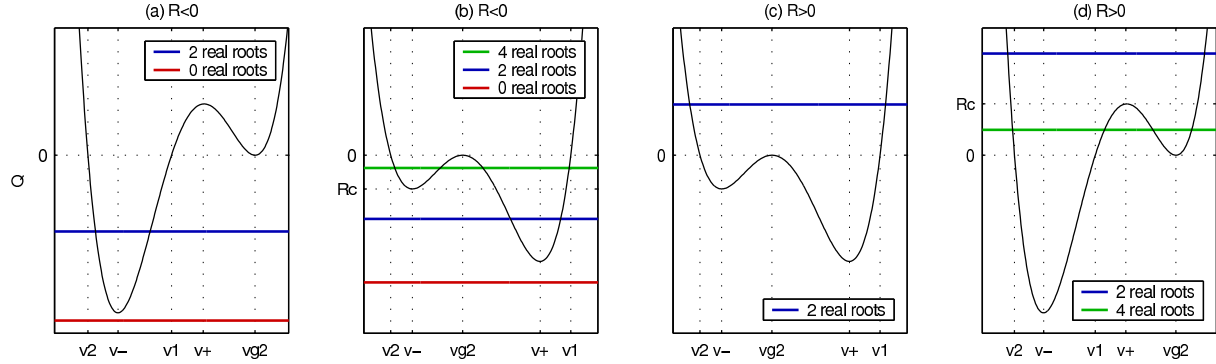


Figure 3: Schematic representations of the possible stability scenarios at $\hat{k} = \hat{k}_{c2}$. Plotted in black in each case is the coupled dispersion function $Q = Q_a(\hat{v}, \hat{k}_{c2})Q_c(\hat{v}, \hat{k}_{c2})$ as a function of \hat{v} , as defined in (45). The horizontal lines denote values of R with differing stability properties.

where \hat{v}_\pm are two of the turning points of $Q = Q_a(\hat{v}, \hat{k}_{c2})Q_c(\hat{v}, \hat{k}_{c2})$, the third being at v_{g2} . When $R < R_c$, $Q_a(\hat{v}, \hat{k}_{c2})Q_c(\hat{v}, \hat{k}_{c2}) = R$ has at least two complex roots, and we can say that coupling is destabilizing, whereas if $R_c < R < 0$ there are four real roots of $Q_a(\hat{v}, \hat{k}_{c2})Q_c(\hat{v}, \hat{k}_{c2}) = R$, and we can say that coupling is stabilizing. But here, in both scenarios, the stability situation may change again as \hat{k} is further reduced below \hat{k}_{c2} .

2. Suppose next that $\omega_1'' > 0$, so that $R > 0$. For sufficiently large \hat{k} , both uncoupled modes are stable, whilst for sufficiently small \hat{k} , both uncoupled modes are unstable. Suppose that as \hat{k} is reduced from infinity, one of the uncoupled modes becomes unstable for some value of \hat{k} , while the other, for this value of \hat{k} is still stable. To be explicit, let us suppose that it is the C -mode which becomes unstable, so that $\hat{k} = \hat{k}_{c2}$ as above. The other case can be treated in the same way. Now at $\hat{k} = \hat{k}_{c2}$ our hypothesis that the A -mode is stable again implies that $\beta^2 > 0$, and once again there are two sub-cases to consider:

- (a) If $|v_{g2} - v_{g1}| \leq \beta$, then the double zero v_{g2} of $Q_c(\hat{v}, \hat{k}_{c2})$ lies in $[\hat{v}_2, \hat{v}_1]$. This scenario is depicted in Figure 3c. Since $R > 0$ and all turning points of $Q = Q_a(\hat{v}, \hat{k}_{c2})Q_c(\hat{v}, \hat{k}_{c2})$ lie in $Q \leq 0$, the coupled system is unstable at $\hat{k} = \hat{k}_{c2}$, and therefore for some $\hat{k} > \hat{k}_{c2}$, and in this sense we can say that coupling is destabilizing. Indeed, in this case the system remains unstable for all $\hat{k} < \hat{k}_c$, where $\hat{k}_c > \hat{k}_{c2}$ is the critical value at which the system first becomes unstable, and is the value of \hat{k} at which the line $Q = R$ is tangent to the graph of $Q = Q_aQ_c$.
- (b) If $|v_{g2} - v_{g1}| > \beta$, then the double zero v_{g2} of $Q_c(\hat{v}, \hat{k}_{c2})$ does not lie in $[\hat{v}_2, \hat{v}_1]$. This scenario is depicted in Figure 3d. Stability at $\hat{k} = \hat{k}_{c2}$ is then once again determined by R_c , defined as before, which is now the value of the single turning point with $Q_aQ_c > 0$. When $R > R_c$, $Q_a(\hat{v}, \hat{k}_{c2})Q_c(\hat{v}, \hat{k}_{c2}) = R$ has two complex roots so coupling is destabilizing, whereas if $0 < R < R_c$ there are four real roots of $Q_a(\hat{v}, \hat{k}_{c2})Q_c(\hat{v}, \hat{k}_{c2}) = R$ and coupling is stabilizing. But here, in both scenarios, the stability situation may change again as \hat{k} is further reduced below \hat{k}_{c2} .

4.5 Summary

We have considered how modulational instabilities of spatially uniform coupled two-wave solutions are predicted by the four weakly nonlinear models of Section 3. As noted in Section 4.2, the non-dispersive nonlinearly coupled envelope equations (21) give an unambiguous prediction of stability for disturbances with \hat{k} of $O(\varepsilon^2)$ on a timescale $\sim \varepsilon^{-2}$. Further, the non-locally coupled NLS equations

(33) give an unambiguous prediction of instability for disturbances with \hat{k} of $O(\varepsilon)$ on a timescale $\sim \varepsilon^{-2}$, whenever $v_{g1} - v_{g2}$ is $O(1)$, and either $\omega_1'' > 0$ or $\omega_2'' > 0$ (the latter is always true here). As shown in Sections 4.3 and 4.4, the coupled NLS equations (35) and (36) give a dispersion relation which is harder to analyse, but we showed that it reproduces the results for disturbances with \hat{k} of $O(\varepsilon)$ or $O(\varepsilon^2)$ in their respective regimes of validity. However, in the context of (36), the coupled NLS dispersion relation also gives predictions which are strictly outside its asymptotic range of validity. Such predictions need to be tested independently, for instance, by numerical simulations of the full unapproximated Sine-Gordon equations. We perform such tests in Section 6, by numerically determining the behaviour of system (3).

5 Modulational instability of four-wave solutions

We now discuss the modulational instability of four-wave solutions. We use the same ideas as in Section 4, except that we restrict our analysis to the non-locally coupled NLS equations, derived for modulations on the long lengthscale $\chi = \varepsilon x$.

5.1 Plane waves

We start by examining the form of spatially uniform coupled plane waves. For such solutions, the non-locally coupled NLS models (33) and (35) reduce to the same system. Looking for solutions of the form

$$A = A_0 e^{i\Omega_a T}, \quad B = B_0 e^{-i\Omega_b T}, \quad C = C_0 e^{i\Omega_c T}, \quad D = D_0 e^{-i\Omega_d T}, \quad (49)$$

we see that a balance is only possible if

$$\Omega_a - \Omega_b = \Omega_c - \Omega_d. \quad (50)$$

Substitution of (49) into (33) or (35) gives

$$\begin{aligned} \Omega_a &= \mu_1(|A_0|^2 + 2|B_0|^2) + \mu_2(|C_0|^2 + |D_0|^2) + \mu_2\phi^*/|A_0|^2, \\ \Omega_b &= \mu_1(2|A_0|^2 + |B_0|^2) + \mu_2(|C_0|^2 + |D_0|^2) + \mu_2\phi^*/|B_0|^2, \\ \Omega_c &= \mu_3(|C_0|^2 + 2|D_0|^2) + \mu_4(|A_0|^2 + |B_0|^2) + \mu_4\phi/|C_0|^2, \\ \Omega_d &= \mu_3(2|C_0|^2 + |D_0|^2) + \mu_4(|A_0|^2 + |B_0|^2) + \mu_4\phi/|D_0|^2, \end{aligned}$$

where

$$\phi = A_0 B_0 C_0^* D_0^*. \quad (51)$$

Thus, for solutions of the form (49), the condition (50) for balance becomes

$$(|A_0|^2 - |B_0|^2) \left(\mu_1 + \frac{\mu_2 C_0 D_0}{A_0 B_0} \right) = (|C_0|^2 - |D_0|^2) \left(\mu_3 + \frac{\mu_4 A_0 B_0}{C_0 D_0} \right). \quad (52)$$

If (52) is satisfied, then we may substitute (49) into (19) to obtain a solution in the form of two pairs of counter-propagating waves,

$$\begin{aligned} \begin{pmatrix} u \\ w \end{pmatrix} &= \varepsilon \left(A_0 e^{i(kx - (\omega_1 - \varepsilon^2 \Omega_a)t)} + B_0 e^{i(kx + (\omega_1 - \varepsilon^2 \Omega_b)t)} \right) \begin{pmatrix} 1 \\ \alpha_1 \end{pmatrix} \\ &\quad + \varepsilon \left(C_0 e^{i(kx - (\omega_2 - \varepsilon^2 \Omega_c)t)} + D_0 e^{i(kx + (\omega_2 - \varepsilon^2 \Omega_d)t)} \right) \begin{pmatrix} 1 \\ \alpha_2 \end{pmatrix} + \text{c.c.} + O(\varepsilon^2). \end{aligned} \quad (53)$$

This solution generalises the linear energy exchange solutions of Section 2.1 by nonlinearly-induced corrections of $O(\varepsilon^2)$ to the frequencies $\omega_{1,2}(k)$ of the linear waves, given by (7). For $\varepsilon \rightarrow 0$, it reduces to the four-wave linear solution (15) if

$$\varepsilon A_0 = \varepsilon B_0 = \frac{|\alpha_2|U}{4(\alpha_1 + |\alpha_2|)}, \quad \varepsilon C_0 = \varepsilon D_0 = \frac{\alpha_1 U}{4(\alpha_1 + |\alpha_2|)}, \quad (54)$$

which clearly satisfies the balance condition (52).

5.2 The non-locally coupled NLS equations: $(v_{g_1} - v_{g_2}) = O(1)$

We first study the instability of the plane-wave solution (49) in the case with v_{g_1} and v_{g_2} both $O(1)$, and $(v_{g_1} - v_{g_2})$ non-zero and $O(1)$. Accordingly we use equations (33), and we look for solutions in the form (41), with corresponding forms for B and D . Neglecting terms quadratic in disturbance amplitude, this yields four linear systems of the form

$$\begin{aligned} \left(\hat{\Omega}_a - \frac{1}{2} \omega_1'' \hat{\kappa}^2 + \mu_1 |A_0|^2 - \frac{\mu_2 \phi^*}{|A_0|^2} \right) a_1 + \mu_1 |A_0|^2 a_2 &= 0, \\ -\mu_1 |A_0|^2 a_1 + \left(\hat{\Omega}_a + \frac{1}{2} \omega_1'' \hat{\kappa}^2 - \mu_1 |A_0|^2 + \frac{\mu_2 \phi}{|A_0|^2} \right) a_2 &= 0. \end{aligned}$$

Note that although this system might appear only to involve $|A_0|$, in fact the terms involving ϕ give a coupling to the other basic state waves via B_0 , C_0 and D_0 , unlike the two-wave case. Each system has an associated dispersion relation of the form

$$\hat{\Omega}_a^2 + \frac{\mu_2}{|A_0|^2} (\phi - \phi^*) \hat{\Omega}_a - \left(\frac{1}{2} \omega_1'' \hat{\kappa}^2 + \frac{\mu_2 \phi}{|A_0|^2} - \mu_1 |A_0|^2 \right) \left(\frac{1}{2} \omega_1'' \hat{\kappa}^2 + \frac{\mu_2 \phi^*}{|A_0|^2} - \mu_1 |A_0|^2 \right) + \mu_1^2 |A_0|^4 = 0.$$

When A_0 , B_0 , C_0 and D_0 all have the same phase, as is the case for (54) for instance, then $\phi = |A_0 B_0 C_0 D_0|$, and the dispersion relation reduces to

$$\hat{\Omega}_a^2 = \left(\frac{1}{2} \omega_1'' \hat{\kappa}^2 - \mu_1 |A_0|^2 + \frac{\mu_2 |B_0 C_0 D_0|}{|A_0|} \right)^2 - \mu_1^2 |A_0|^4. \quad (55)$$

Reverting to dimensional variables using (43) gives

$$\left(\hat{\omega}_a - \hat{k} v_{g_1} \right)^2 = \left(\frac{1}{2} \omega_1'' \hat{\kappa}^2 - (1 - r_a) \mu_1 |\varepsilon A_0|^2 \right)^2 - \mu_1^2 |\varepsilon A_0|^4, \quad r_a = \frac{\mu_2}{\mu_1} \left| \frac{B_0 C_0 D_0}{A_0^3} \right|, \quad (56)$$

with corresponding forms for $\hat{\omega}_b$, $\hat{\omega}_c$ and $\hat{\omega}_d$. Although equations (55) and (56) have a similar form to their two-wave counterparts (42) and (44), there are important differences. For instance, consider the instability of the A -mode, as given by (56).

When $\omega_1'' > 0$, (44) shows that for the two-wave solution a maximum growth rate of $s_* = \mu_1 |\varepsilon A_0|^2$ is achieved by the A -mode when $\hat{k}^2 = \hat{k}_*^2 = 2\mu_1 |\varepsilon A_0|^2 / |\omega_1''| > 0$. However, for the four-wave solution, instability of the A -mode is instead determined by the parameter r_a , and only if $r_a = 0$ are the two-wave results recovered. If $0 < r_a \leq 1$, then (56) is minimised at $\hat{k}^2 = \hat{k}_*^2(1 - r_a)$, so that the disturbance wavenumber of the most unstable A -mode is reduced, although the growth rate remains s_* . If $r_a > 1$, (56) is instead minimised at $\hat{k} = 0$, with value $s_*^2(r_a^2 - 2r_a) > -s_*^2$. Therefore, if $1 < r_a < 2$ the most unstable A -mode occurs at $\hat{k} = 0$ with a reduced growth rate $s < s_*$, whilst if $r_a \geq 2$ the A -mode is stable. Thus, a two-wave solution can yield an instability in the A -mode whilst a corresponding four-wave solution does not.

When $\omega_1'' < 0$, (44) shows that the two-wave solution does not lead to an instability in the A -mode. However, when $r_a \geq 1$, (56) is minimised at $\hat{k}^2 = (r_a - 1)\hat{k}_*^2$, leading to an instability in the A -mode with growth rate s_* . If $0 < r_a < 1$, (56) is instead minimised at $\hat{k} = 0$, with value $s_*^2(r_a^2 - 2r_a) > -s_*^2$, leading to an instability in the A -mode with a reduced growth rate $s < s_*$. Thus, a four-wave solution can yield an instability in the A -mode whilst a corresponding two-wave solution does not.

There are corresponding conclusions for the B mode, and for the C and D -modes (for which $\omega_2'' > 0$), and the overall stability of (49) will be determined by the most unstable of these four modes. Although the possible stabilising and destabilising effects outlined above are of interest, we do not consider the details any further here.

5.3 The non-locally coupled NLS equations: $(v_{g_1} - v_{g_2}) = O(\varepsilon)$

We now turn to the case with v_{g_1} and v_{g_2} both $O(1)$, but $(v_{g_1} - v_{g_2}) = O(\varepsilon)$. Accordingly we use equations (35), and we look for solutions in the form

$$A(\bar{\eta}, T) = A_0(T)(1 + a_1 e^{i(\hat{\kappa}\bar{\eta} - \hat{\Omega}_{ac}T)} + a_2^* e^{-i(\hat{\kappa}\bar{\eta} - \hat{\Omega}_{ac}^*T)}),$$

$$C(\bar{\eta}, T) = C_0(T)(1 + c_1 e^{i(\hat{\kappa}\bar{\eta} - \hat{\Omega}_{ac}T)} + c_2^* e^{-i(\hat{\kappa}\bar{\eta} - \hat{\Omega}_{ac}^*T)}),$$

with corresponding forms for B and D . Neglecting terms quadratic in disturbance amplitude leaves a coupled system in A and C , and a coupled system in B and D . The latter system reduces to the former with the equivalence $A \leftrightarrow B, C \leftrightarrow D, \bar{\xi} \leftrightarrow \bar{\eta}, \hat{\Omega}_{bd} \leftrightarrow -\hat{\Omega}_{ac}$, so it is sufficient to just consider the behaviour of the coupled A, C system, say, which reduces to solving

$$\begin{aligned} \left(\hat{\Omega}_{ac} + \hat{\kappa}\Delta - \frac{1}{2}\omega_1''\hat{\kappa}^2 + \mu_1|A_0|^2 - \frac{\mu_2\phi^*}{|A_0|^2} \right) a_1 + \mu_1|A_0|^2 a_2 + \mu_2 \left(|C_0|^2 + \frac{\phi^*}{|A_0|^2} \right) c_1 + \mu_2|C_0|^2 c_2 &= 0, \\ -\mu_1|A_0|^2 a_1 + \left(\hat{\Omega}_{ac} + \hat{\kappa}\Delta + \frac{1}{2}\omega_1''\hat{\kappa}^2 - \mu_1|A_0|^2 + \frac{\mu_2\phi}{|A_0|^2} \right) a_2 - \mu_2|C_0|^2 c_1 - \mu_2 \left(|C_0|^2 + \frac{\phi}{|A_0|^2} \right) c_2 &= 0, \\ \mu_4 \left(|A_0|^2 + \frac{\phi}{|C_0|^2} \right) a_1 + \mu_4|A_0|^2 a_2 + \left(\hat{\Omega}_{ac} - \hat{\kappa}\Delta - \frac{1}{2}\omega_2''\hat{\kappa}^2 + \mu_3|C_0|^2 - \frac{\mu_4\phi}{|C_0|^2} \right) c_1 + \mu_3|C_0|^2 c_2 &= 0, \\ -\mu_4|A_0|^2 a_1 - \mu_4 \left(|A_0|^2 + \frac{\phi^*}{|C_0|^2} \right) a_2 - \mu_3|C_0|^2 c_1 + \left(\hat{\Omega}_{ac} - \hat{\kappa}\Delta + \frac{1}{2}\omega_2''\hat{\kappa}^2 - \mu_3|C_0|^2 + \frac{\mu_4\phi^*}{|C_0|^2} \right) c_2 &= 0. \end{aligned}$$

Thus, as in Section 4.4, the dispersion relation may be obtained by setting a 4×4 determinant to be zero. However, in contrast to Section 4.4, the presence of the terms involving ϕ makes it hard to derive analytically a quartic equation for $\hat{\Omega}_{ac}$. Thus, we find the roots numerically for a given parameter set, by calling an eigenvalue routine for the above system, giving $\hat{\Omega}_{ac}$ directly.

6 Numerical simulations

We perform numerical simulations of the original system (3) of coupled Sine-Gordon equations to examine the accuracy and validity of the theoretical predictions of instability derived in Sections 4 and 5. In our previous study [10] we verified that the modulational instability of two-wave solutions is well described by the non-locally coupled NLS equations, over a wide parameter range. Here, we make a more detailed comparison between the predictions of this theory, those of the coupled NLS equations, and the numerical results, for the instability of both two-wave and four-wave solutions. Although our emphasis will be on verifying the growth rate of modulational instabilities, we will also comment on the structure of the solutions when any instabilities reach maximum amplitude.

6.1 The numerical method

Since the plane wave solutions and the modulational instabilities we analyse are spatially periodic, it is natural to use a Fourier basis for the x -dependence of u and w . Then, denoting a quantity $q(x, t)$ as $\sum_{j \geq 0} \tilde{q}_j(t) e^{ijx} + \text{c.c.}$, where j is one of the numerically resolved wavenumbers, we write (3) as the first order system

$$\begin{pmatrix} \tilde{u} \\ \tilde{u}_t \\ \tilde{w} \\ \tilde{w}_t \end{pmatrix}_t = \begin{pmatrix} 0 & 1 & 0 & 0 \\ -(\delta^2 + j^2) & 0 & \delta^2 & 0 \\ 0 & 0 & 0 & 1 \\ 1 & 0 & -(1 + c^2 j^2) & 0 \end{pmatrix} \begin{pmatrix} \tilde{u} \\ \tilde{u}_t \\ \tilde{w} \\ \tilde{w}_t \end{pmatrix} + \tilde{N}_j(t) \begin{pmatrix} 0 \\ \delta^2 \\ 0 \\ -1 \end{pmatrix}, \quad (57)$$

where the terms $\tilde{N}_j(t)$ originate from $N(x, t) = (u - w) - \sin(u - w)$. We solve this using a split-step scheme, a method which has frequently been applied to such nonlinear wave equations. Neglecting the nonlinear terms in (57), i.e. those involving \tilde{N} , we obtain a linear system that can be updated exactly,

since given \tilde{u} , \tilde{u}_t , \tilde{w} and \tilde{w}_t at time t , and $\omega_{1,2}(j)$, we can write down explicitly the solution of the linear system at time $t + \Delta t$. Similarly, neglecting the linear terms in (57), i.e. those not involving \tilde{N} , we obtain a system in which \tilde{u} and \tilde{w} are constant, so that \tilde{u}_t and \tilde{w}_t can be trivially updated by using the value of \tilde{N} at time t . This latter property relies on the second derivatives with respect to t in the governing equations. By combining these two steps in a sequence of appropriately chosen fractional steps, one may obtain a method of any order (as explained, for instance, in section 2 of [39]). For the simulations to be presented, we use a fourth order scheme with a time-step in the range 0.025 to 0.1, with 96 to 768 points in the x -direction, and the term \tilde{N} evaluated pseudospectrally. The nonlinear scheme then conserves energy to a high degree – typically to within $10^{-6}\%$. If the nonlinear terms are neglected, then the scheme exactly resolves linear dynamics, within roundoff error.

For initial conditions, we take either (8) or (14) which lead to the two-wave or four-wave exchange solutions (39) and (54) respectively, with wavenumber k and amplitude parameter U . The domain width l is then restricted by the need to choose $l = 2\pi n/k$, where n is a positive integer. To trigger any instabilities, we add background noise to u and w , at a level at least 1000 times smaller than the amplitude parameter U . In unstable cases, we identify a modulational instability of wavenumber \hat{k} by calculating the energy in pairs of sideband modes with wavenumbers $k \pm \hat{k}$. To do this we consider the quantity

$$E_{side|m}(t) = \tilde{E}_{k+\hat{k}} + \tilde{E}_{k-\hat{k}}, \quad \hat{k} = 2\pi m/l, \quad \text{with } m \text{ a positive integer,} \quad (58)$$

corresponding to the energy in the m -th pair of numerically resolved sideband modes. Here \tilde{E}_j is the energy, calculated according to (6), when u and w are replaced by their Fourier components with wavenumber j . Initially, $E_{side|m}(t)$ typically grows exponentially for one or more m , permitting growth rates to be calculated for the corresponding wavenumbers $\hat{k} = 2\pi m/l$.

To check the relevance of these growth rates, we also distinguish a disturbance energy. Although the linear solution projects solely onto wavenumber k , the unperturbed nonlinear plane wave solution under consideration projects onto wavenumbers $(2n+1)k$, for all non-negative integers n . Therefore we define an energy associated with the plane wave and its nonlinear harmonics

$$E_{plane} = \sum_{n \geq 0} \tilde{E}_{(2n+1)k}, \quad (59)$$

and an energy associated with the disturbance field

$$\hat{E} = \sum_{j \neq (2n+1)k} \tilde{E}_j. \quad (60)$$

An overall disturbance growth rate can then be calculated by analysing \hat{E} . Typically, the growth rate of one pair of sideband modes approximately equals the growth rate of \hat{E} , so that we can identify with some certainty which sideband pair yields the most relevant modulational instability.

This method has been tested by calculating the growth rate for the modulational instability of a one-wave solution at $c = 1$ and $\varepsilon \ll 1$, when stability is determined by that of a corresponding uncoupled Sine-Gordon equation. Calculated growth rates typically agree with the well-known theoretical prediction (e.g. [37]) to at least four significant figures.

6.2 Instability at small amplitude

We first consider the instability of small amplitude plane-wave solutions, for which the individual wave amplitudes εA_0 , εB_0 , εC_0 and εD_0 are all less than 0.1. We reduce the parameter regime to manageable proportions by only considering waves that satisfy the full-exchange condition (11). Then, according to (39) and (54), and recalling from Section 2 that $\alpha_1 = -\alpha_2 = \delta^{-1}$ for full exchange parameters, we have $\varepsilon A_0 = \varepsilon C_0 = U/4$ for two-wave solutions, and $\varepsilon A_0 = \varepsilon B_0 = \varepsilon C_0 = \varepsilon D_0 = U/8$ for four-wave solutions. Here U is the maximum amplitude of u in the linear solution, although the maximum amplitude of w is U/δ .

The results are summarised in Table 1. Numerically determined growth rates \hat{s}_n are given for modulational instability at just a single wavenumber \hat{k}_n , corresponding to a relatively strong instability in each case. For the two-wave runs U has been chosen so that the maximum value of u or w in the linear solution is 0.2, so that the values of εA_0 and εC_0 are 0.025 or 0.05. For the four-wave runs, U is twice that of the corresponding two-wave simulation, so that the maximum value of u or w in the linear solutions is now 0.4. However, the individual wave amplitudes are the same in both cases, and in this sense the runs are closely related.

	c	1.5	1.1	0.5	$\sqrt{3}$	$\sqrt{2}/3$	$\sqrt{1.5}$
Wave Parameters	δ	1.5	1.1	0.5	3	0.5	3
	k	1	1	1	2	1.5	4
	v_{g_1}	1.228	1.049	0.722	1.265	0.884	1.066
	v_{g_2}	0.746	0.607	0.472	1	0.722	0.945
	$v_{g_1} - v_{g_2}$	0.483	0.441	0.249	0.265	0.162	0.121
2-wave results	U	0.2	0.2	0.1	0.2	0.1	0.2
	\hat{k}_n	1/12	0.1	0.05	1/15	0.075	0.125
	\hat{s}_n	0.00248	0.00268	0.00116	0.00224	0.00091	0.00168
	\hat{s}_c	0.00249	0.00268	0.00116	0.00221	0.00091	0.00167
	\hat{s}_{ac}	0.00249	0.00268	0.00116	0.00223	0.00091	0.00168
4-wave results	U	0.4	0.4	0.2	0.4	0.2	0.4
	\hat{k}_n	1/12	0.1	0.05	1/15	0.075	0.125
	\hat{s}_n	0.00243	0.00263	0.00116	0.00196	0.00089	0.00149
	$\hat{s}_c = \hat{s}_d$	0.00248	0.00268	0.00120	0.00202	0.00089	0.00154
	$\hat{s}_{ac} = \hat{s}_{bd}$	0.00248	0.00268	0.00119	0.00200	0.00089	0.00152

Table 1: Numerically determined growth rates \hat{s}_n for small amplitude solutions.

We first discuss the two-wave results. There are two theoretical predictions for the growth rate. The first comes from the non-locally coupled NLS equations, valid when $\hat{k} = O(\varepsilon)$ and $(v_{g_1} - v_{g_2}) = O(1)$. This theory predicts the existence of two possible modes of instability, one evident as growth in wave amplitude A and the other as growth in C , and can be diagnosed from (44). Since $\omega_1'' < 0$ for all the parameters considered here, $\hat{\omega}_a$ is real and hence A is always stable. Thus, we need only calculate the growth rate of C , which we denote by $\hat{s}_c = \text{Im}(\hat{\omega}_c)$. The second prediction comes from the coupled system (45), valid when $\hat{k} = O(\varepsilon)$ and $(v_{g_1} - v_{g_2}) = O(\varepsilon)$, or equivalently from the coupled NLS equations. This predicts growth of a coupled mode in A and C , and we denote this growth rate by $\hat{s}_{ac} = \text{Im}(\hat{\omega}_{ac})$.

As shown in Table 1, both \hat{s}_c and \hat{s}_{ac} are in good agreement with \hat{s}_n for all the parameters considered. Indeed, it is perhaps surprising that \hat{s}_c is a good approximation for the final one or two cases, when $v_{g_1} - v_{g_2}$ is apparently small. However, one can also see that \hat{s}_c and \hat{s}_{ac} are almost equal for these cases. This seems to be because for a wide range of full exchange parameters, such as those in Table 1, at least one of μ_2 , μ_4 , ω_1'' and ω_2'' is small. Thus, for small amplitude conditions, the coupling term R in (45) is not important, so that even when $v_{g_1} - v_{g_2}$ is small the growth rate is approximately determined by the uncoupled instability in C .

Turning to the four-wave results, we once again have two predictions for the growth rate. The first is the uncoupled growth rate for the C and D modes, which have the same growth rate \hat{s}_c . Even though $\hat{s}_a = \hat{s}_b$ can be positive, $\hat{s}_c > \hat{s}_a$ for all the parameters in Table 1. The second prediction, denoted by \hat{s}_{ac} , is no longer derived from the coupled NLS equations, but rather from the non-locally coupled NLS equations, valid when $\hat{k} = O(\varepsilon)$, with $(v_{g_1} - v_{g_2}) = O(\varepsilon)$, and v_{g_1}, v_{g_2} both $O(1)$, as described in Section 5.3. It now describes a coupled instability in A and C , or an equivalent instability in B and D , with the same growth rate.

As shown in Table 1, there is now generally a small discrepancy between the numerically determined growth rate and the best theoretical prediction. We speculate that this is an effect of the wave amplitude – recall that in the linear solution the maximum amplitude reached by u or w is 0.4, twice that of the two-wave simulations. This point will be clarified in the next section.

6.3 Instability at moderate amplitude

We now consider how \hat{s}_n and the functions \hat{s}_c , \hat{s}_{ac} change as U is increased, for three different parameter sets. We first discuss a full-exchange case with $c = \delta = 1.5$, $k = 1$, for which $v_{g1} = 1.23$, $v_{g2} = 0.75$, so that $v_{g1} - v_{g2} = 0.48$. The nonlinear interaction coefficients are $\mu_1 = 0.003$, $\mu_2 = 0.13$, $\mu_3 = 1.00$, $\mu_4 = 0.08$, and $\omega_1'' = -0.31$, $\omega_2'' = 0.73$. The results are shown in Figure 4. For the two-wave case, given in Figure 4a, the theoretical predictions \hat{s}_c and \hat{s}_{ac} are almost indistinguishable. For small U they closely follow \hat{s}_n , whilst as U is increased the differences between the predictions and \hat{s}_n grow. The four-wave results, given in Figure 4b, show the same type of behaviour. However, note how the four-wave predictions are different from the corresponding two-wave predictions (at $U/2$, as shown by the dotted line), particularly at small \hat{k} .

Although it is apparent from Figure 4 that both $|\hat{s}_c - \hat{s}_n|$ and $|\hat{s}_{ac} - \hat{s}_n|$ vanish as $U \rightarrow 0$, we would really like to show that the relative error of the predictions vanishes as $U \rightarrow 0$, and hence that \hat{s}_c and \hat{s}_{ac} have the correct limiting behaviour at small amplitude. Therefore, given a numerically determined growth rate \hat{s}_n , for a theoretical prediction \hat{s}_p we introduce a relative error

$$e_r(\hat{s}_p) = \frac{\hat{s}_n - \hat{s}_p}{\hat{s}_n}. \quad (61)$$

The quantity $|e_r(\hat{s}_c)|$ is shown in Figures 4c,d for the runs of Figures 4a,b. In both the two-wave and four-wave cases one can see that the relative error does vanish as $U \rightarrow 0$. Indeed, one can show in each case that $e_r \approx U^2 \times \text{some function of } (\hat{k}/U)$. Note that the relative errors for the two-wave and four-wave cases are of the same order of magnitude when comparing by U (rather than by the individual wave amplitude εC_0).

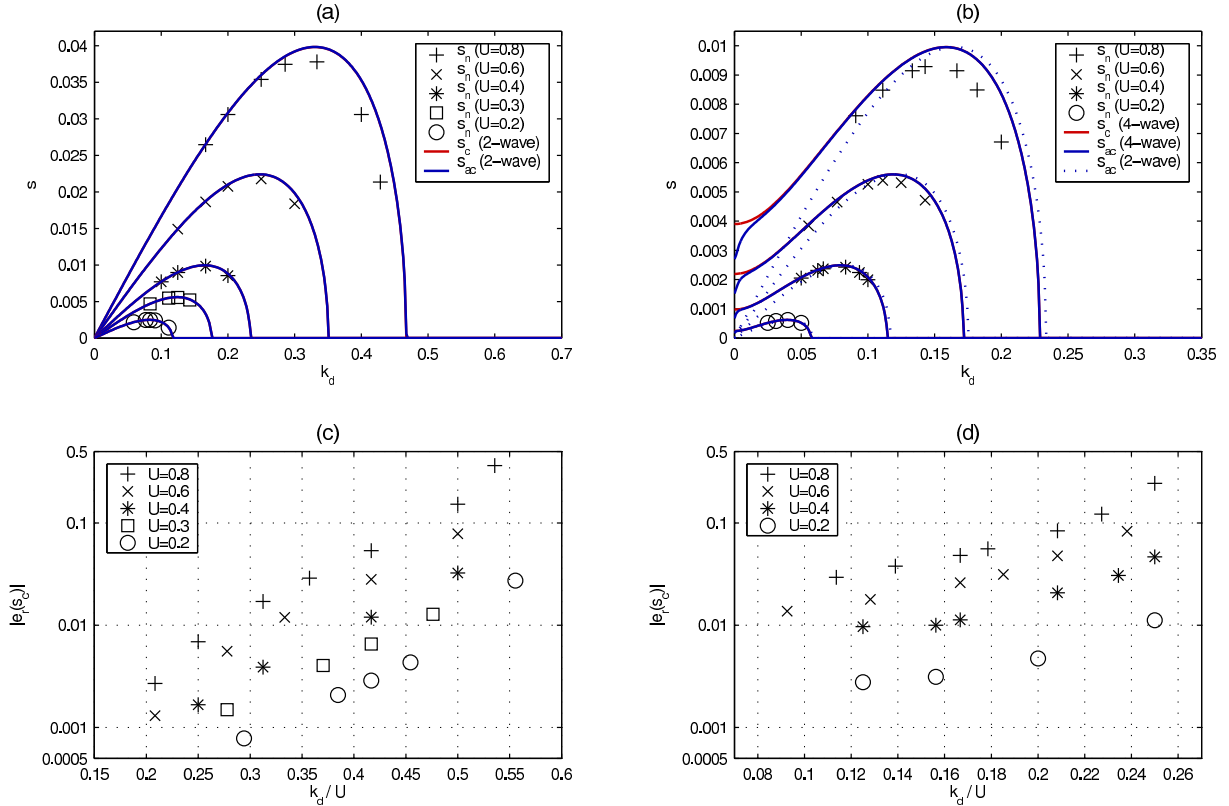


Figure 4: Numerically determined growth rates and theoretical predictions at $c = \delta = 1.5$, $k = 1$ as a function of disturbance wavenumber $k_d = \hat{k}$. (a) Two-wave results. (b) Four-wave results. (c) The quantity $|e_r(\hat{s}_c)|$ for the two-wave prediction \hat{s}_c , as defined in (61). (d) The quantity $|e_r(\hat{s}_c)|$ for the four-wave prediction \hat{s}_c .

For the two-wave cases we have already noted that \hat{s}_c and \hat{s}_{ac} are almost indistinguishable. However, is \hat{s}_{ac} more accurate than \hat{s}_c ? Perhaps, for the larger amplitude cases in Figure 4a, (35) is a more suitable model than (33) because the wave amplitudes are now of the same order as $(v_{g_1} - v_{g_2}) = 0.48$? Or perhaps the coupled NLS model (36) is necessarily more accurate than the non-locally coupled NLS model (33)? At least for these parameters, the answer to all three of these questions is no, since $|\hat{s}_n - \hat{s}_c|$ is marginally smaller than $|\hat{s}_n - \hat{s}_{ac}|$. Further, from (48) we calculate that $|v_{g_2} - v_{g_1}| > \beta$ for all the two-wave cases, so that at the wavenumber \hat{k}_{c_2} where the uncoupled C-mode becomes unstable the coupled NLS equations predict the destabilizing scenario 1(a) of Section 4.4. However, one can clearly see in the large amplitude cases of Figure 4a that there is a stabilization at $\hat{k} = \hat{k}_{c_2}$, rather than a destabilization.

The second case we discuss, also a full exchange solution, has $c = \sqrt{1.5}$, $\delta = 3$, $k = 4$, for which $v_{g_1} = 1.07$, $v_{g_2} = 0.95$, so that $v_{g_1} - v_{g_2} = 0.12$. The nonlinear interaction coefficients are $\mu_1 = 0.05$, $\mu_2 = 0.38$, $\mu_3 = 0.67$, $\mu_4 = 0.34$, and $\omega_1'' = -0.12$, $\omega_2'' = 0.19$. The results are shown in Figure 5. For the two-wave case, both \hat{s}_c and \hat{s}_{ac} offer a good approximation to \hat{s}_n . At small amplitudes, \hat{s}_c and \hat{s}_{ac} are almost identical, as expected, and as shown in Figure 6c, \hat{s}_c shows the desired convergence properties as $U \rightarrow 0$. At larger amplitudes, where perhaps we enter the regime with $U \sim (v_{g_1} - v_{g_2})$, there are differences between \hat{s}_c and \hat{s}_{ac} , and here \hat{s}_{ac} is a better approximant. Indeed, $|v_{g_2} - v_{g_1}| > \beta$ as defined in (48), so that the coupled NLS models predict the destabilizing scenario 1(a) of Section 4.4 with $\hat{s}_n > 0$ at $\hat{k} = \hat{k}_{c_2}$, which is verified at $U = 0.6$, for instance. For the four-wave case, there are clear differences between \hat{s}_c and \hat{s}_{ac} even at small amplitudes when \hat{k} is also small. To obtain relative errors comparable to the two-wave case, it is now necessary to use the prediction \hat{s}_{ac} , as shown in Figure 6d. In both two-wave and four-wave cases, note that $|e_r|$ increases with \hat{k} at fixed U , which is perhaps associated with a breakdown in the scale assumption implicit in the weakly nonlinear theory leading to \hat{s}_c and \hat{s}_{ac} .

Differences between the theoretical predictions \hat{s}_c and \hat{s}_{ac} can be highlighted by considering parameters such that $v_{g_1} = v_{g_2}$. Therefore we consider the case $c = 2/3$, $\delta = 3/4$, $k = 3/2$, for which $v_{g_1} = v_{g_2} = 0.71$. The nonlinear interaction coefficients are $\mu_1 = 0.07$, $\mu_2 = 0.29$, $\mu_3 = 0.60$, $\mu_4 = 0.57$, and $\omega_1'' = -0.18$, $\omega_2'' = 0.37$. These do not satisfy the full exchange condition (11). For two-wave solutions, (39) gives $\varepsilon A_0 = 0.13U$, $\varepsilon C_0 = 0.37U$, and for four-wave solutions (54) gives $\varepsilon A_0 = \varepsilon B_0 = 0.065U$, $\varepsilon C_0 = \varepsilon D_0 = 0.18U$. According to (9) and (15), the maximum amplitude of w in the linear solution is $1.17U$.

Results for these parameters are shown in Figure 6. For both two-wave and four-wave cases, there are now significant differences between \hat{s}_c and \hat{s}_{ac} . Although \hat{s}_c gives moderate agreement with \hat{s}_n , it completely misses the second tongue of instability at large \hat{k} , and $|e_r(\hat{s}_c)|$ does not decrease with U . However, \hat{s}_{ac} does have the correct qualitative behaviour. To assess its quantitative performance, we consider the relative error $e_r(\hat{s}_{ac})$, as shown in Figures 6c,d. Because \hat{s}_{ac} can be greater or less than \hat{s}_n , we plot $e_r(\hat{s}_{ac})$ (which may be positive or negative) rather than $|e_r(\hat{s}_{ac})|$ as before, allowing the form of the curves to be fully appreciated. For the two-wave case, the points with $\hat{k}/U \leq 5/6$, which includes the region of maximum growth, show good convergence as $U \rightarrow 0$. For $\hat{k}/U > 5/6$, convergence is no longer clear, although the actual behaviour could be masked by the limited discrete resolution of e_r . Nevertheless, errors here remain at about 10%. For the four-wave case, the points with $\hat{k}/U \leq 0.32$, which includes the region of maximum growth, also show good convergence as $U \rightarrow 0$. For $\hat{k}/U > 0.32$, it appears that $e_r(\hat{s}_{ac})$ assumes a form independent of U , with no decrease as $U \rightarrow 0$, although errors here still remain at about 10%.

For the two-wave cases we have $\beta > |v_{g_2} - v_{g_1}| = 0$ as defined in (48), so that we lie in scenario 1(b) of Section 4.4. One can then verify that $R < R_c$ for all the cases in Figure 6a, so that the coupled NLS models predict a destabilization at $\hat{k} = \hat{k}_{c_2}$, as is clearly the case at each U . Note this destabilization at $\hat{k} = \hat{k}_{c_2}$ is not inconsistent with the vanishing of \hat{s}_{ac} (and \hat{s}_n) for some $\hat{k} < \hat{k}_{c_2}$, as noted at the end of scenario 1(b). This twin-tongued growth rate structure is typical for two-wave cases with $|v_{g_1} - v_{g_2}| \ll 1$.

For the four-wave cases, the numerical simulations also show the existence of a second tongue of instability with a higher disturbance wavenumber than those shown in Figure 6. This appears at

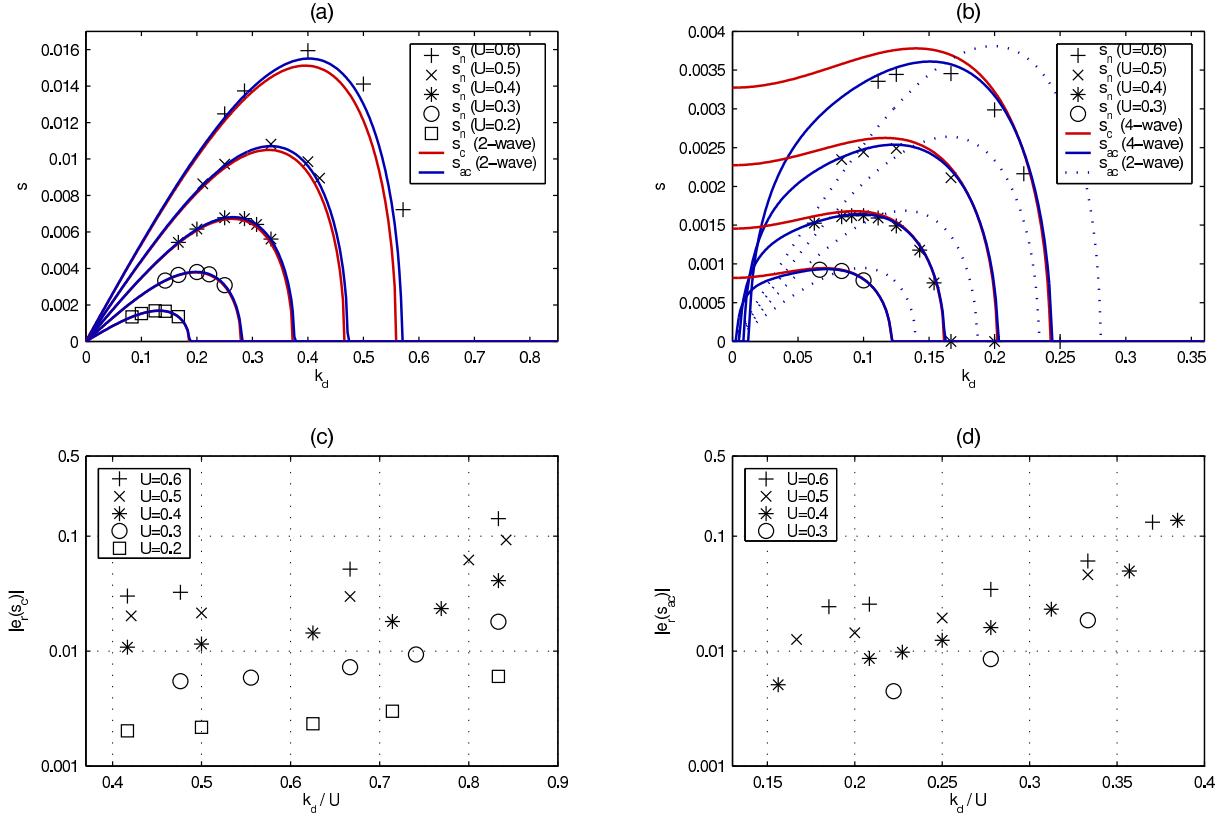


Figure 5: Numerically determined growth rates and theoretical predictions at $c = \sqrt{1.5}$, $\delta = 3$, $k = 4$ as a function of disturbance wavenumber $k_d = \hat{k}$. (a) Two-wave results. (b) Four-wave results. (c) The quantity $|e_r(\hat{s}_c)|$ for the two-wave prediction \hat{s}_c , as defined in (61). (d) The quantity $|e_r(\hat{s}_{ac})|$ for the four-wave prediction \hat{s}_{ac} .

$U = 0.3$ as an instability with $\hat{s}_n = 0.00256$ and $\hat{k} = 15/34$, and at $U = 0.4$ as an instability with $\hat{s}_n = 0.00483$ and $\hat{k} = 3/7$, and in both cases is the strongest instability observed at that amplitude U . Such instabilities are not predicted by any of our theories. Indeed, even though this is an instability of a weakly nonlinear plane wave, the modulating wavenumber $\hat{k} \approx k/3$, so that it does not correspond to a long spatial modulation of the type considered here.

6.4 Character of the instability at finite amplitude

In our previous study of the instability of two-wave solutions [10], we showed how the energy exchange between u and w in the plane-wave solution can have a counterpart during the finite amplitude stage of a modulational instability. We now examine further the nature of this finite amplitude energy exchange, and extend the discussion to the four-wave case and to the long-time behaviour of the system.

In order to make clear conclusions, we consider a restricted class of scenarios. First, we restrict the plane-wave parameters to $c = \delta$ and $k = 1$, all of which satisfy the full exchange condition (11). Then, for c and δ of $O(1)$, $v_{g1} - v_{g2} \approx 0.5$, and we lie in a stability regime like that of Figure 4. Second, we restrict the computational geometry so that just one of the numerically resolved sidebands is unstable. We achieve this by taking $l \approx 2\pi/\hat{k}_{c*}$, where \hat{k}_{c*} is the most unstable wavenumber associated with the prediction \hat{s}_c , as determined by (44) or by the C-mode version of (56). We then obtain an evolution in which the initial plane-wave structure becomes modulated on the lengthscale of the computational domain, with no possibility of an interaction between modulational instabilities of two different wavelengths.

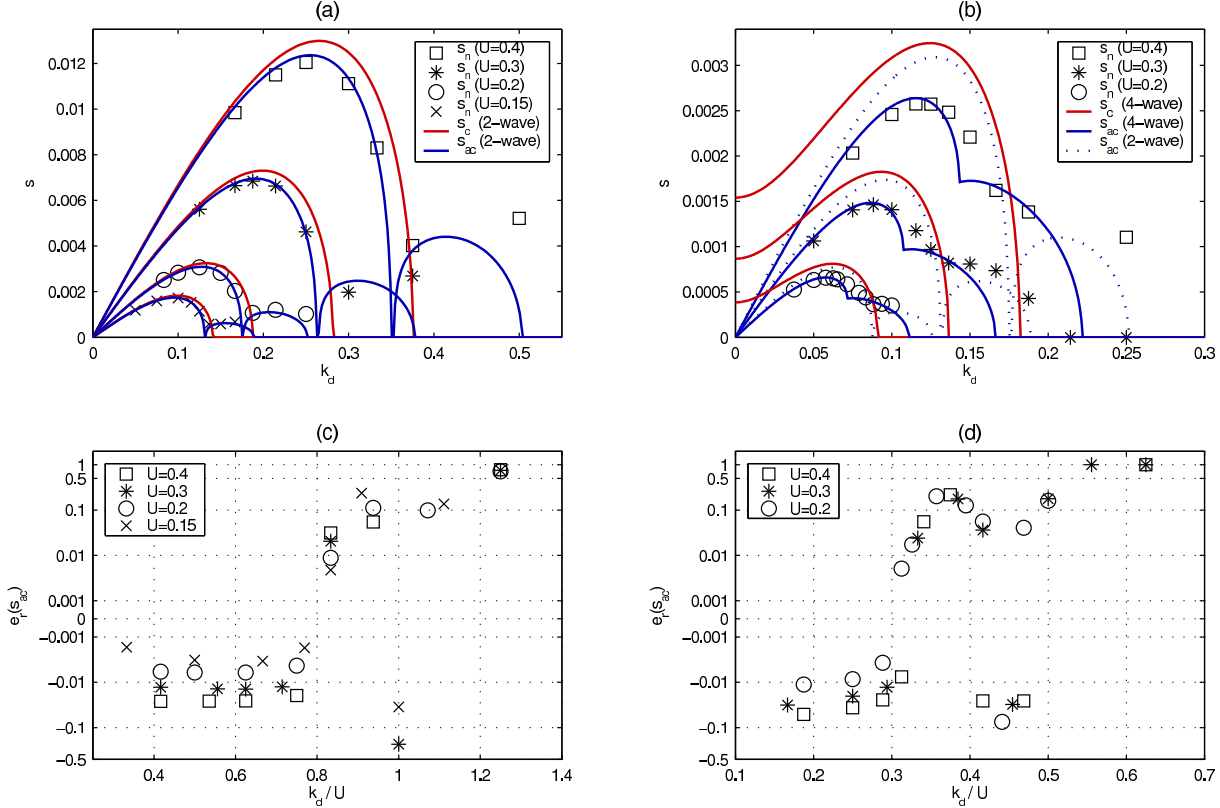


Figure 6: Numerically determined growth rates and theoretical predictions at $c = 2/3$, $\delta = 3/4$, $k = 3/2$ as a function of disturbance wavenumber $k_d = \hat{k}$. (a) Two-wave results. (b) Four-wave results. (c) The quantity $e_r(\hat{s}_{ac})$ for the two-wave prediction \hat{s}_{ac} , as defined in (61). (d) The quantity $e_r(\hat{s}_{ac})$ for the four-wave prediction \hat{s}_{ac} .

We start by discussing an important special case, that of $c = \delta = 1$. Here, the system (3) decouples into a Sine-Gordon equation and a linear wave equation, and, therefore, is integrable [28]. As a consequence, the modulational instability of plane-wave solutions shows a recurrence, similar to the famous Fermi–Pasta–Ulam recurrence [41]. We view this behaviour by considering the time evolution of three quantities: E_{plane} , as defined in (59), representing the strength of the plane-wave and its nonlinear harmonics; $E_{\text{side}|1}$, as defined in (58), representing the strength of the modulational instability in the first sideband pair, with disturbance wavenumber $\hat{k} = 2\pi/l$; and $E - E_{\text{plane}} - E_{\text{side}|1}$, representing the contribution from other wavenumbers.

These quantities are shown in the top row of Figure 7, during the instability of a two-wave solution at $c = \delta = 1$, with $U = 0.4$ and $l = 8\pi$. One can clearly see an almost periodic recurrence, with most of the energy either in E_{plane} , or $E_{\text{side}|1}$. In the second row, one can see how E is partitioned between u , w and the coupling, as defined in (6), whilst in the third and four rows one can see $u(x, t)$ and $w(x, t)$ respectively (the complete computational domain is shown). At first the plane-wave solution has a periodic energy exchange, which is almost complete between E_u and E_w , as approximately described by (12) and (13). At the first minimum in E_{plane} , near $t = 1300$, there is still a periodic energy exchange between u and w , although the exchange is no longer almost complete, i.e. E_u and E_w no longer almost vanish periodically. Further, at this time $u(x, t)$ and $w(x, t)$ are strongly modulated on the largest resolved scale, and the large amplitude behaviour pulses between u and w . Thus, the almost complete energy exchange with spatially uniform structures initially observed is modified in the nonlinear regime to an incomplete energy exchange with structures localized on the lengthscale of the computational domain. Note that these same two scenarios alternate, in line with the recurrence of E_{plane} and $E_{\text{side}|1}$. One can see how $u(x, t)$ and $w(x, t)$ return almost to their initial plane-wave

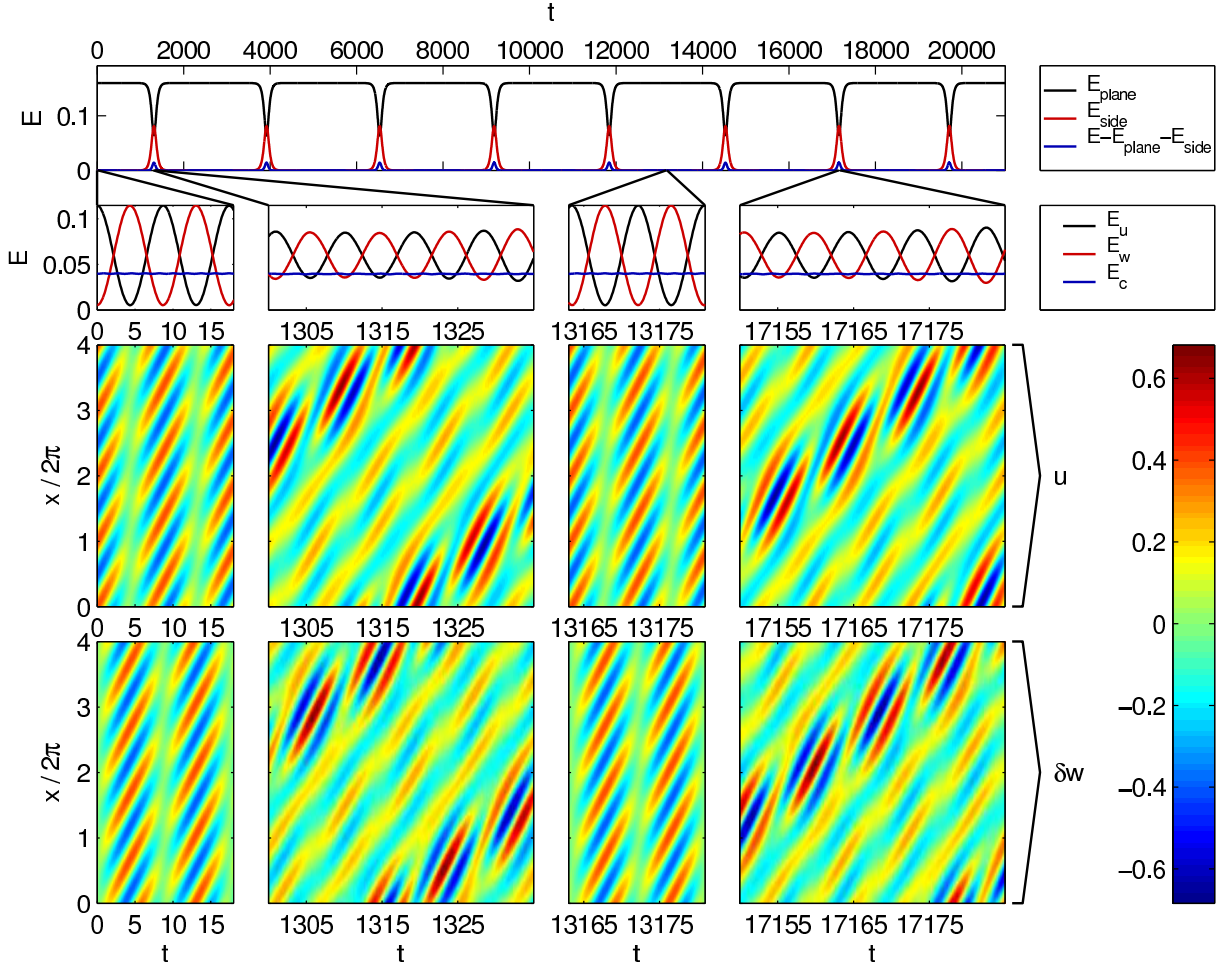
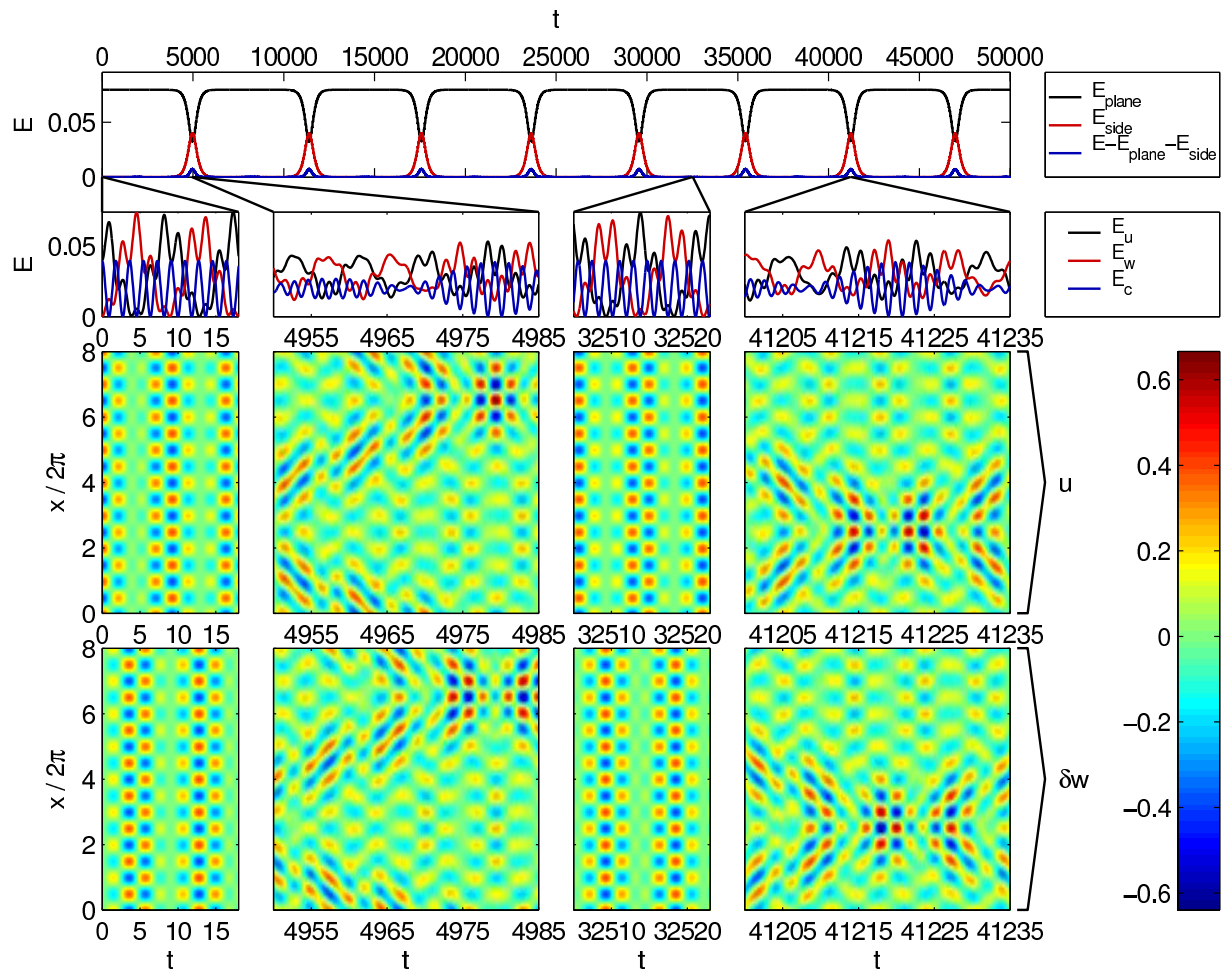


Figure 7: Time evolution of a two-wave solution at $c = \delta = 1$, $k = 1$, $U = 0.4$, with $l = 8\pi$.

form when $E_{side|1}$ is minimised, near $t = 13,170$ for instance, whilst the pulsing modulations return when $E_{side|1}$ is maximised, near $t = 17,150$ for instance.

The four-wave case at $c = \delta = 1$ with $U = 0.4$ is similar, as shown in Figure 8. Once again there is an almost periodic recurrence in E_{plane} and $E_{side|1}$. However, the partitioning of E between the components E_u , E_w and E_c is more complicated than in the two-wave case, with rapid oscillations in each component superimposed on a slower exchange between E_u and E_w . Once again, when E_{plane} is maximised the slow exchange between E_u and E_w is almost complete, whilst when $E_{side|1}$ is maximised the slow exchange becomes incomplete. The general pattern of an almost periodic sequence of alternating exchange patterns remains, from approximately uniform wavetrains to localized structures and back, and so on.

A natural question to ask is to what extent similar behaviour occurs when $c \neq 1$. Shown in Figure 9 are results of corresponding simulations at $c = \delta = 1.01$ and $c = \delta = 1.1$, with $U = 0.4$ in both cases. For the two-wave cases, shown in panels (a) and (c), the period of the recurrence now varies, although the character of each recurrence event appears to remain almost the same. For the four-wave cases, shown in panels (b) and (d), the character of the recurrence events now varies, but the evolution is still predominantly characterized by an exchange between E_{plane} and $E_{side|1}$. Thus both two-wave and four-wave cases exhibit an imperfect recurrence, which we might expect since, for c close to 1, the equations are close to being an integrable system. Interestingly, the system (3) with c close to 1 has been used to model some dynamical processes in the DNA [24, 25], where such energy exchange processes could, potentially, play an important role.


 Figure 8: Time evolution of a four-wave solution at $c = \delta = 1$, $k = 1$, $U = 0.4$, with $l = 16\pi$.

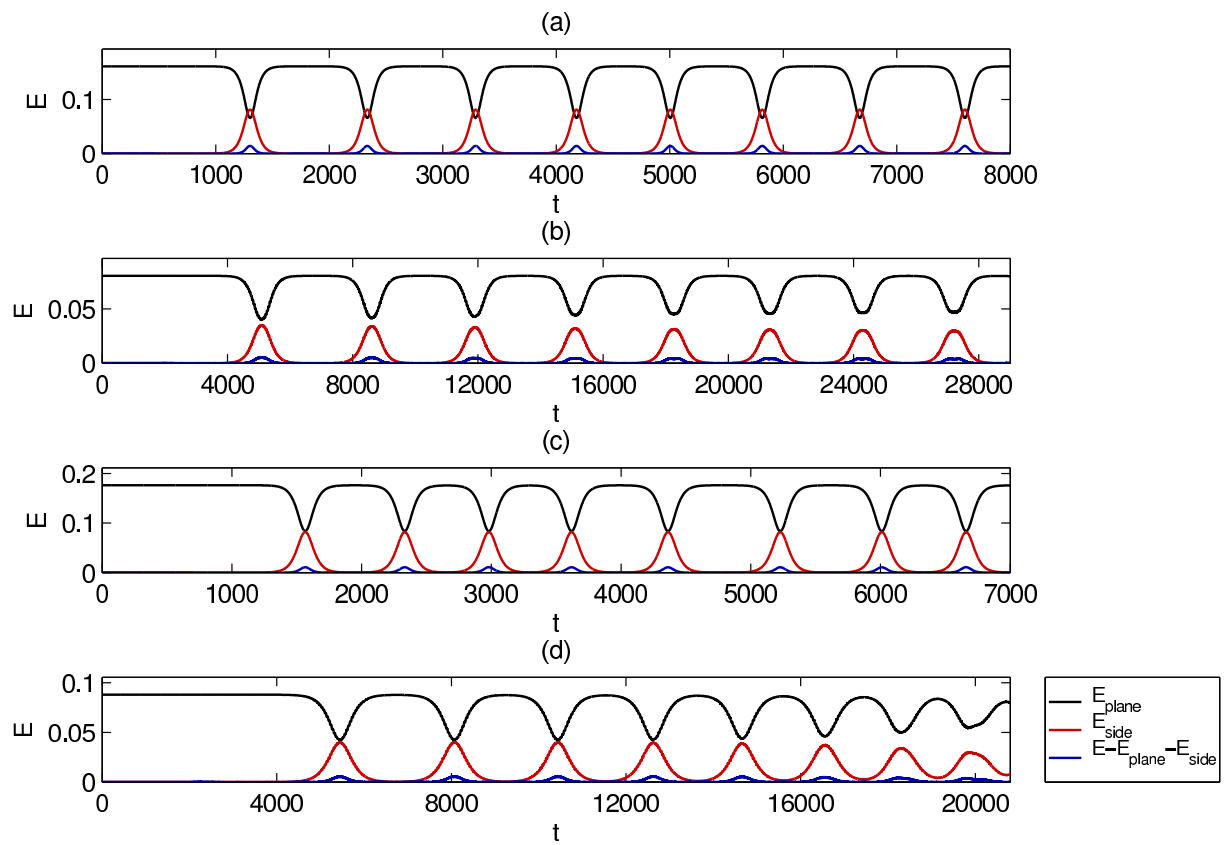
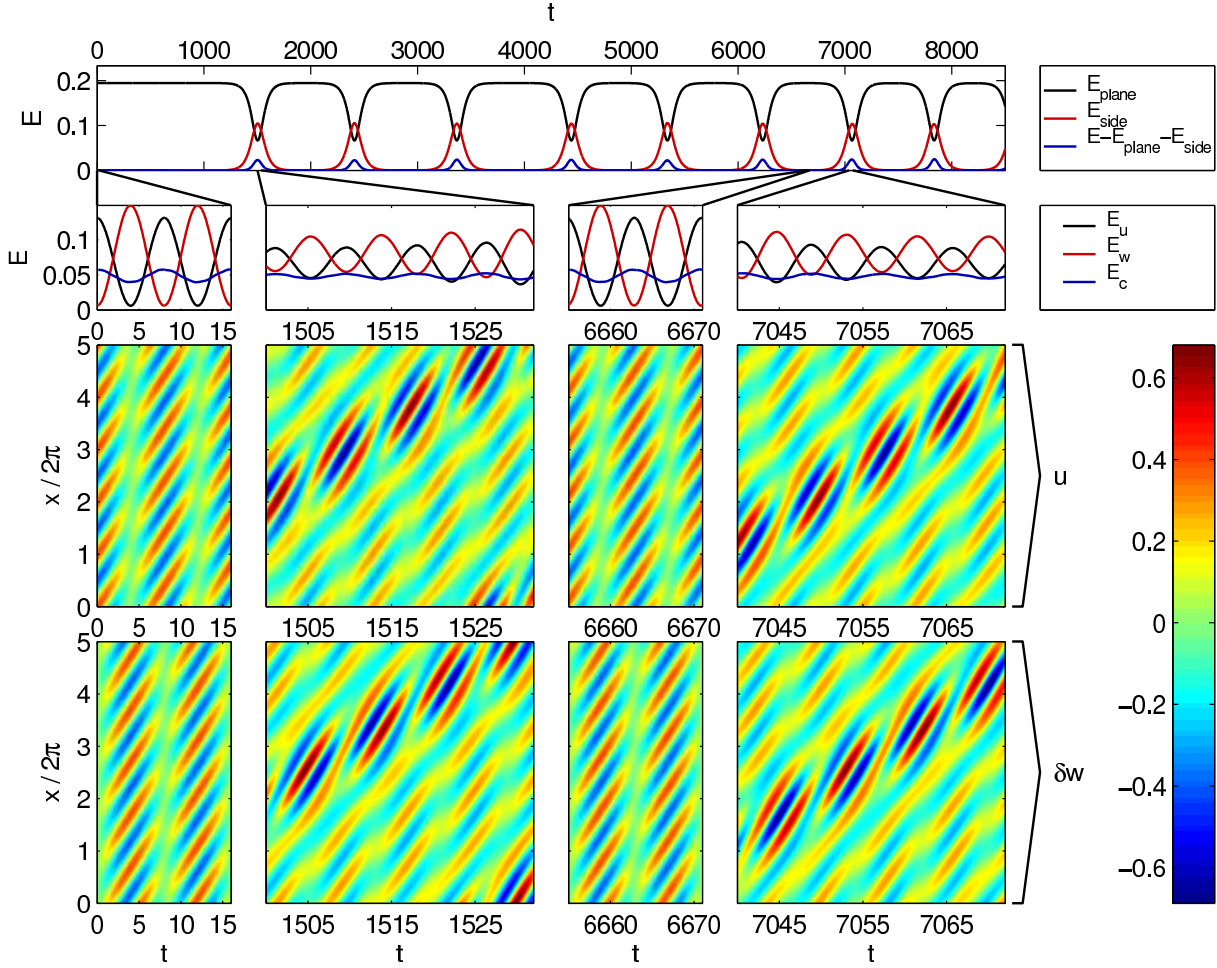


Figure 9: Time evolution of solutions with $k = 1$ and $U = 0.4$: (a) a two-wave solution at $c = \delta = 1.01$, with $l = 8\pi$; (b) a four-wave solution at $c = \delta = 1.01$, with $l = 16\pi$; (c) a two-wave solution at $c = \delta = 1.1$ with $l = 8\pi$; (d) a four-wave solution at $c = \delta = 1.1$ with $l = 16\pi$.


 Figure 10: Time evolution of a two-wave solution at $c = \delta = 1.2$, $k = 1$ and $U = 0.4$, with $l = 10\pi$.

Although the recurrence becomes imperfect when $c \neq 1$, the alternating pattern of approximately uniform wavetrains and localized structures remains. Shown in Figures 10 and 11 are the results of two-wave and four-wave simulations at $c = \delta = 1.2$, with $U = 0.4$. The two-wave case of Figure 10 still looks remarkably similar to that of Figure 7, taken at $c = \delta = 1$. However, in the four-wave case of Figure 11, the recurrence breaks down around $t = 13,000$, only to reappear later in the evolution. Further, during the second sequence of recurrence events, around $t = 17,000$, the alternating pattern of approximately uniform wavetrains and localized structures reappears. For instance, around $t = 17,100$ one can see that the solution only has a small spatial modulation, whilst around $t = 17,730$ the solution has a spatial character almost identical to that of the first recurrence event around $t = 5680$. More remarkably, note from the second row of Figure 11 how even the details of the exchange between E_u , E_w and E_c are almost identical around $t = 5680$ and $t = 17,730$.

However, for larger values of $c = \delta$, evolutions which might be described as recurrent become rare, and typically the solutions display a more irregular behaviour. To illustrate this, we show results for the case $c = \delta = 1.5$. Shown in Figure 12 is the evolution of a two-wave solution, with $U = 0.4$ and $l = 12\pi$, whilst shown in Figure 13 is the evolution a four-wave solution, with $U = 0.4$ and $l = 24\pi$. (One can pick out these parameters in Figure 4, and verify that they correspond to relatively strong instabilities in each case). In the two-wave case, at large times the solution loses much of the character of the earlier recurrence. The four-wave case displays an irregular, imperfect recurrence, the character of which does seem to be similar to the earlier events.

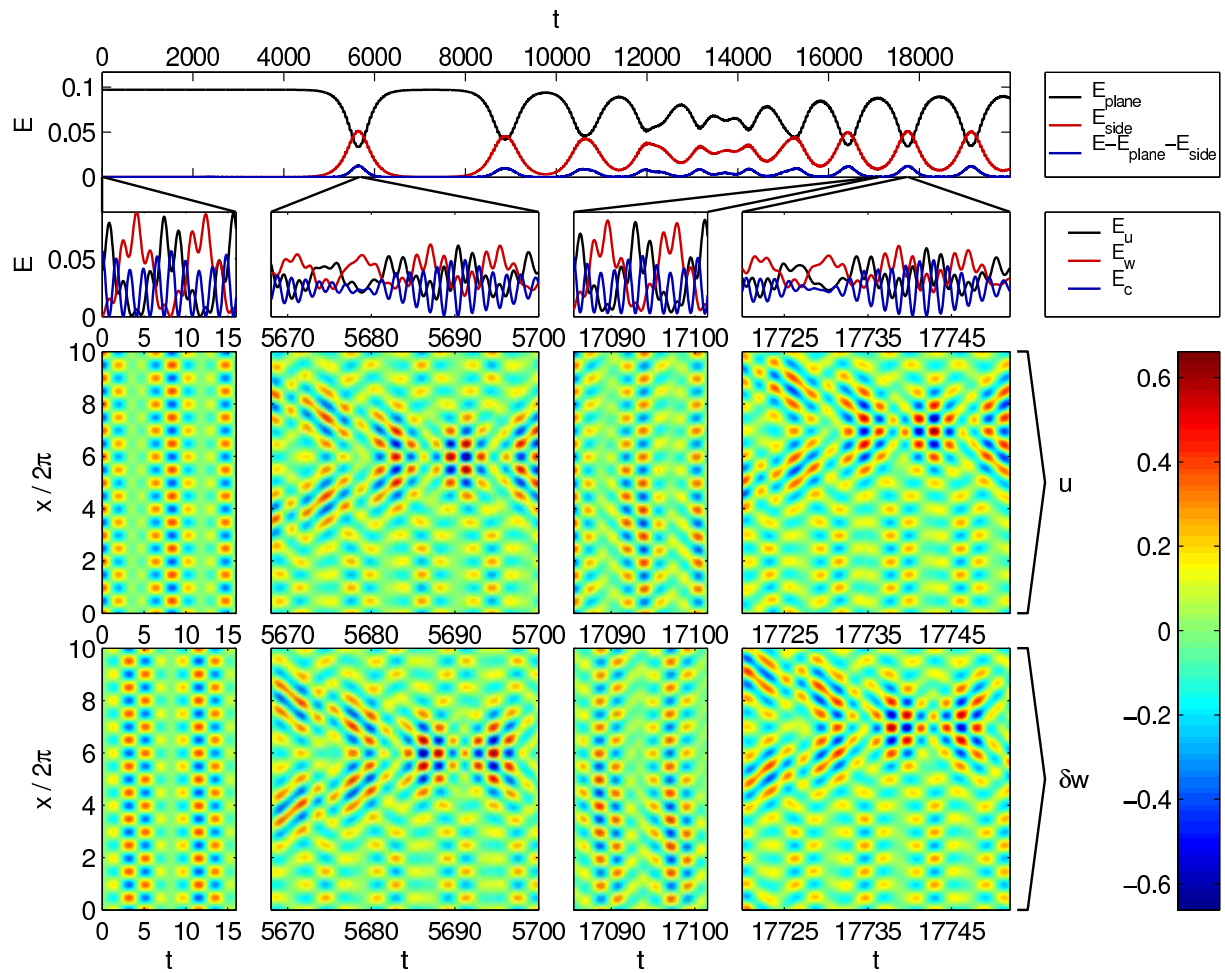


Figure 11: Time evolution of a four-wave solution at $c = \delta = 1.2$, $k = 1$ and $U = 0.4$, with $l = 20\pi$.

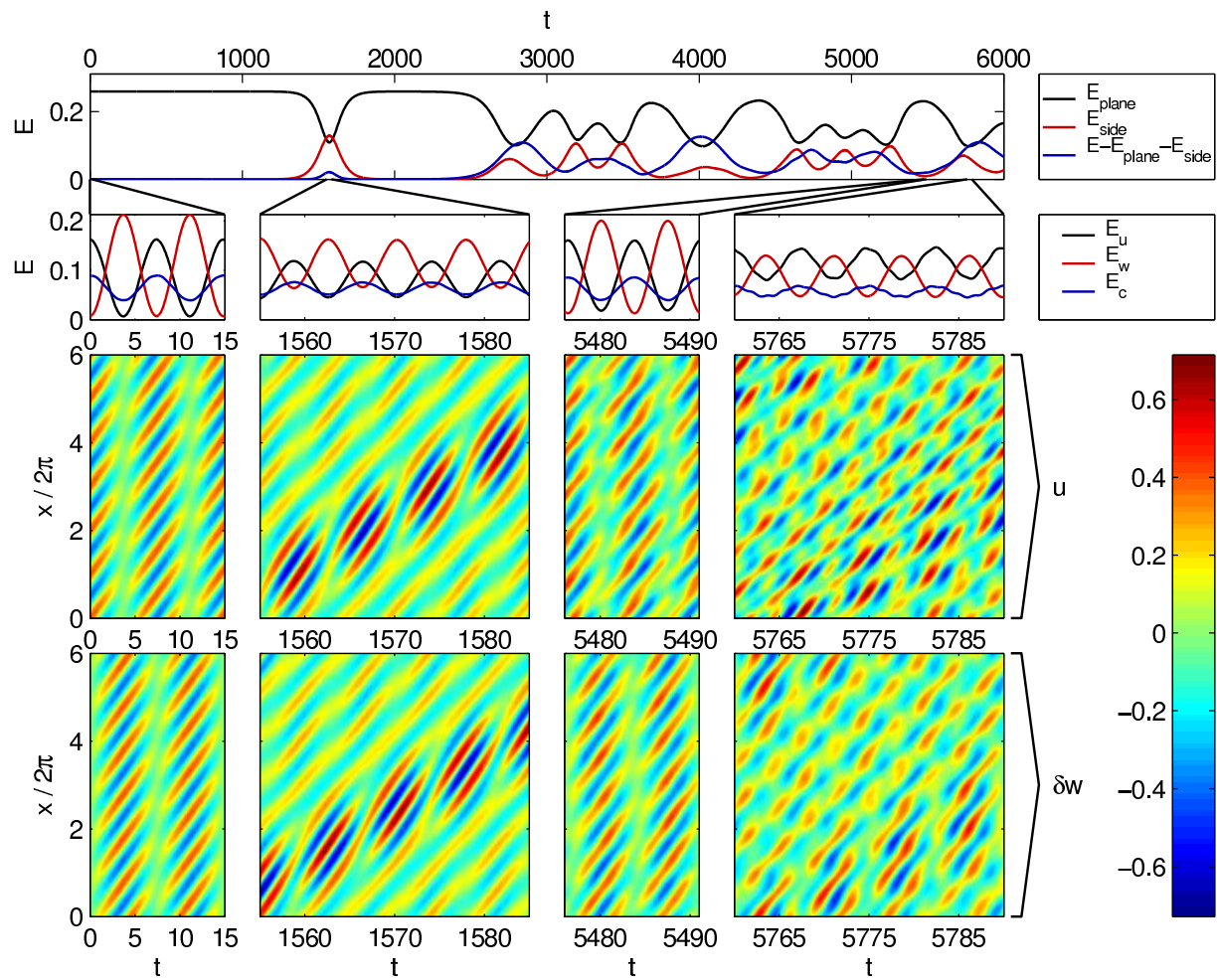
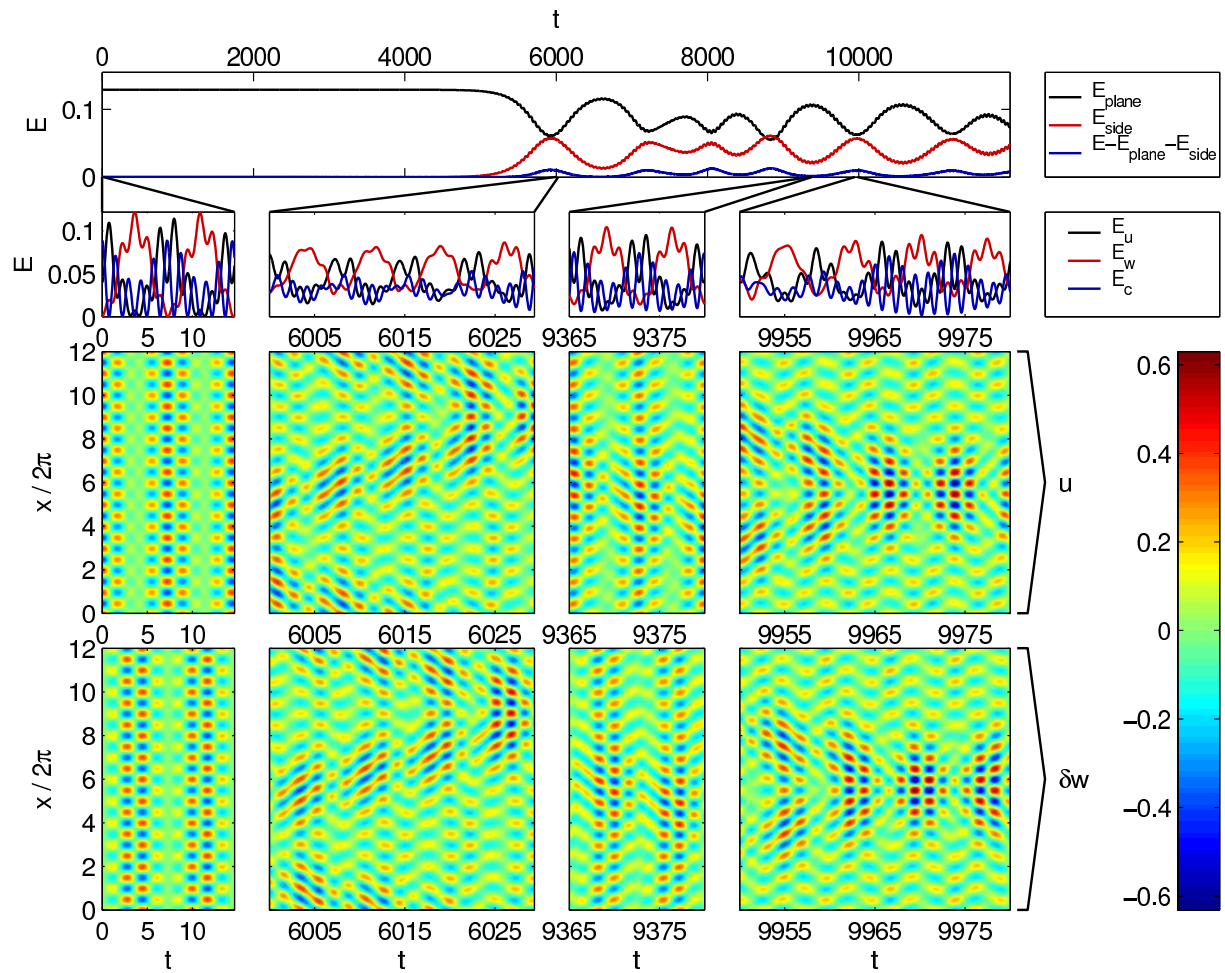


Figure 12: Time evolution of a two-wave solution at $c = \delta = 1.5$, $k = 1$ and $U = 0.4$, with $l = 12\pi$.


 Figure 13: Time evolution of a four-wave solution at $c = \delta = 1.5$, $k = 1$ and $U = 0.4$, with $l = 24\pi$.

7 Conclusion

We have studied the nonlinear dynamics of two pairs of counter-propagating waves within the framework of a two-component system of coupled Sine-Gordon equations (3). Using both analytical and numerical methods, we considered the evolution of spatially periodic solutions characterized by a single dominant wavenumber k , focussing on the possible modulational instability of spatially uniform plane-wave solutions. We concentrated on a particular class of plane-wave solutions corresponding to an energy exchange between the two physical components of the system, and for these solutions we noted how modulational instabilities can lead to a modification of the energy exchange, and to the formation of localized structures.

The analytical results were based upon asymptotic multiple-scales expansions for the evolution of weakly nonlinear wave packets, which reduced (3) to coupled equations for the evolution of four spatially varying wave amplitudes. However, the form of the amplitude equations depends crucially upon the assumed length-scale of the wave packets *vis-a-vis* the wave amplitude parameter $\varepsilon \ll 1$ and the group velocities v_{g1} and v_{g2} . In Section 3 we derived two classes of evolution equations for the regime relevant to this system with v_{g1} and v_{g2} both of $O(1)$: a set (21) of non-dispersive nonlinearly coupled envelope equations for modulations on a lengthscale $\sim \varepsilon^{-2}$, and two sets (33) and (35) of non-locally coupled NLS equations for modulations on a lengthscale $\sim \varepsilon^{-1}$, according as to whether $(v_{g1} - v_{g2}) = O(1)$ or $O(\varepsilon)$. We have also considered a set (36) of coupled NLS equations with asymptotically weak dispersion, which formally includes each of the other models as different asymptotic reductions. However, it is not clear which set of amplitude equations most efficiently captures the nonlinear dynamics of interest.

The stability of plane-wave solutions involving only a single pair of waves was considered in Section 4, whilst the stability of plane-wave solutions involving two pairs of counter-propagating waves was considered in Section 5. In both cases the non-locally coupled NLS equations for the regime with $(v_{g1} - v_{g2}) = O(1)$ lead to quadratic dispersion relations for the disturbance frequency, enabling simple stability conclusions to be reached. One interesting feature of these results is that a coupled four-wave solution can be stable even whilst one or more of the four component waves can be unstable in isolation. This is in contrast to coupled two-wave solutions, for which stability is equivalent to that of the two component waves in isolation. For the regime with $(v_{g1} - v_{g2}) = O(\varepsilon)$, the non-locally coupled NLS equations lead to quartic dispersion relations for the disturbance frequency. The coupled NLS equations lead to a quartic dispersion relation for two-wave solutions, and to an eighth-order dispersion relation for four-wave solutions, although the latter was not evaluated here.

Numerical methods were used to solve the fully nonlinear Sine-Gordon equations (3) in a periodic domain, using plane-wave initial conditions, as described in Section 6. A major issue was to assess the performance of the stability predictions obtained from the different weakly nonlinear models. For cases with $(v_{g1} - v_{g2}) = O(1)$, the quadratic dispersion relations of the non-locally coupled NLS equations give good predictions: relative errors are about 2 % when the amplitude parameter $U = 0.5$, and these decrease with U . For two-wave cases, the quartic dispersion relation of the coupled NLS equations gives no more accurate predictions, even at large amplitudes. As $|v_{g1} - v_{g2}|$ decreases, the quadratic dispersion relations become less accurate, and the quartic dispersion relations of the non-locally coupled NLS regime with $(v_{g1} - v_{g2}) = O(\varepsilon)$, or equivalently of the coupled NLS equations in the two-wave case, become more useful. For cases where the group velocities are very close or equal, the quadratic dispersion relations of the non-locally coupled NLS equations no longer even predict qualitatively the correct form of the dispersion curve, and a quartic dispersion relation must be used. The region of maximum growth is then well described, with relative errors decreasing with U , although at larger disturbance wavenumbers convergence appears to be poor and relative errors are about 10 %. In some four-wave cases there is an additional dominant short-wavelength instability, which does not correspond to a long spatial modulation of the type considered theoretically, and is not predicted by any of our theories.

The numerical simulations also enabled us to examine the long-time evolution of modulational instabilities. For the energy exchange parameters of interest, the initial solutions are spatially uniform plane-waves with an almost complete energy exchange between the components, whilst later in the

evolution the solutions can become spatially localized with an incomplete energy exchange. Further, when the system is close to the integrable case at $c = 1$, the time evolution is distinguished by a remarkable almost periodic sequence of energy exchange scenarios, with spatial patterns alternating between approximately uniform wavetrains and localized structures. As c moves away from 1, the time evolution becomes more disordered.

Although the whole of this study was performed for a two-component set of coupled Sine-Gordon equations, we would expect similar phenomena to arise in a wide class of nonlinear wave systems. Thus, in addition to applications to multi-component systems such as those mentioned in the Introduction, processes of the type considered here should arise in other physical systems which can support several wave modes. For instance, an interesting example might be energy exchange between nonlinear internal waves in a layered, or continuously stratified, fluid.

Acknowledgments

We are thankful to E.S. Benilov, E. Knobloch and A.V. Mikhailov for useful and stimulating discussions.

References

- [1] Handbook of Plasma Physics, Vols. 1 and 2: Basic Plasma Physics, Ed. A.A. Galeev and R.N. Sudan (North-Holland Publ. Company, 1983–1984).
- [2] G.P. Agrawal, Nonlinear fiber optics (Academic press, 2001).
- [3] Y.S. Kivshar and G.P. Agrawal, Optical Solitons – From Fibers to Photonic Crystals (Academic Press, London, 2003).
- [4] H.C. Yuen and B.M. Lake, Nonlinear dynamics of deep-water gravity waves, *Adv. Appl. Mech.* **22** (1982) 67–229.
- [5] C. Martel, E. Knobloch and J.M. Vega, Dynamics of counter-propagating waves in parametrically forced systems, *Phys. D* **137** (2000) 94–123.
- [6] C. Martel, J.M. Vega and E. Knobloch, Dynamics of counter-propagating waves in parametrically driven systems: dispersion vs advection, *Phys. D* **174** (2003) 198–217.
- [7] F.J. Mancebo, J.M. Vega, Standing wave description of nearly conservative, parametrically driven waves in extended systems, *Phys. D* **197** (2004) 346–363.
- [8] T.J. Bridges and F.E. Laine-Pearson, Nonlinear counterpropagating waves, multisymplectic geometry, and the instability of standing waves, *SIAM J. Appl. Math.* **64** (2004) 2096–2120.
- [9] M. Onorato, D. Ambrosi, A.R. Osborne and M. Serio, Interaction of two quasi-monochromatic waves in shallow water, *Phys. Fluids* **15** (2003) 3871–3874.
- [10] S.D. Griffiths, R.H.J. Grimshaw and K.R. Khusnutdinova, The influence of modulational instability on energy exchange in coupled Sine-Gordon equations, *Theoret. and Math. Phys.* **137** (2003) 1448–1458.
- [11] G. Iooss, P. Plotnikov, J. Toland, Standing waves on infinite depth, *C. R. Math. Acad. Sci. Paris* **338** (2004) 425–431.
- [12] J. Porter, M. Silber, Resonant triad dynamics in weakly damped Faraday waves with two-frequency forcing, *Phys. D* **190** (2004) 93–114.
- [13] A.C. Newell, Solitons in mathematics and physics (SIAM, 1985).

- [14] V.E. Zakharov, Stability of periodic waves of finite amplitude on the surface of a deep fluid, *J. Appl. Mech. Tech. Phys.* **2** (1968) 190–194.
- [15] T.B. Benjamin and J.E. Feir, The disintegration of wave trains on deep water, *J. Fluid Mech.* **27** (1967) 417–430.
- [16] E. Knobloch and J. De Luca, Amplitude equations for travelling wave convection, *Nonlinearity* **3** (1990) 975–980.
- [17] E. Knobloch and J.D. Gibbon, Coupled NLS Equations for counter propagating waves in systems with reflection symmetry, *Phys. Lett. A* **154** (1991) 353–356.
- [18] R.D. Pierce and C.E. Wayne, On the validity of mean-field amplitude equations for counter-propagating wavetrains, *Nonlinearity* **8** (1995) 769–779.
- [19] M.G. Forest, D.W. McLaughlin, D.J. Muraki and O.C. Wright, Nonfocusing instabilities in coupled, integrable nonlinear Schrödinger PDEs, *J. Nonlinear Sci.* **10** (2000) 291–331.
- [20] M.G. Forest and O.C. Wright, An integrable model for stable:unstable wave coupling phenomena, *Phys. D* **178** (2003) 173–189.
- [21] I.Sh. Akhatov, V.A. Baikov and K.R. Khusnutdinova, Non-linear dynamics of coupled chains of particles, *J. Appl. Math. Mech.* **59** (1995) 353–361.
- [22] K.R. Khusnutdinova, Nonlinear waves in a bi-layer and coupled Klein–Gordon equations, in A.B. Movchan ed., *IUTAM Symposium on Asymptotics, Singularities and Homogenization in Problems of Mechanics, Solid Mechanics and Its Applications*, Vol. 113, Kluwer Academic Publishers (2003) 537–546.
- [23] K.R. Khusnutdinova and V.V. Silberschmidt, Lattice modelling of nonlinear waves in a bi-layer with delamination, *Proc. Estonian Acad. Sci. Phys. Math.* **52** (2003) 63–75.
- [24] S. Yomosa, Soliton excitations in deoxyribonucleic acid (DNA) double helices, *Phys. Rev. A* **27** (1983) 2120–2125.
- [25] L.V. Yakushevich, *Nonlinear Physics of DNA* (Wiley, Chichester, 1998).
- [26] T.A. Kontorova and Ya.I. Frenkel, On the theory of plastic deformation and twinning I, II, *Zh. Eksp. Teor. Fiz.* **8** (1938) 89–95; 1340–1368.
- [27] O.M. Braun and Yu.S. Kivshar, Nonlinear dynamics of the Frenkel-Kontorova model, *Phys. Rep.* **306** (1998) 1–108.
- [28] K.R. Khusnutdinova and D.E. Pelinovsky, On the exchange of energy in coupled Klein-Gordon equations, *Wave Motion* **38** (2003) 1–10.
- [29] L.I. Mandelshtam, *Lectures on the theory of oscillations* (Nauka, Moscow, 1972).
- [30] V.I. Arnold, *Mathematical methods of classical mechanics* (Springer, New York, 1989).
- [31] G. Kopidakis, S. Aubry, and G.P. Tsironis, Targeted energy transfer through discrete breathers in nonlinear systems, *Phys. Rev. Lett.* **87** (2001) 165501.
- [32] P. Maniadis, G. Kopidakis, S. Aubry, Classical and quantum targeted energy transfer between nonlinear oscillators, *Phys. D* **188** (2004) 153–177.
- [33] P.J. Olver, *Applications of Lie groups to differential equations*, (Springer-Verlag, New York, 1986).
- [34] D.J. Benney and A.C. Newell, The propagation of nonlinear wave envelopes, *Stud. Appl. Math.* **46** (1967) 133–139.

- [35] M.J. Ablowitz and H. Segur, Solitons and the Inverse Scattering Transform (SIAM, Philadelphia, 1981).
- [36] M. Abramowitz and I.A. Stegun, Handbook of mathematical functions (Nauka, Moscow, 1979).
- [37] S. Fauve, Pattern forming instabilities, in Hydrodynamics and nonlinear instabilities, Ed. C. Godrèche, P. Manneville, (Cambridge University Press, Cambridge, 1998).
- [38] O. Thual, S. Douady, S. Fauve, Parametric instabilities, in Instabilities and nonequilibrium structures II, Ed. E. Tirapegui, D. Villarroel (Dordrecht, Kluwer Academic, 1989).
- [39] G.M. Muslu and H.A. Erbay, A split-step Fourier method for the Complex Modified Korteweg-de Vries Equation, *Comput. Math. Appl.* **45** (2002) 503–514.
- [40] B. Tan and J.P. Boyd, Stability and long time evolution of the periodic solutions to the two coupled nonlinear Schrödinger equations, *Chaos Solitons Fractals* **12** (2001) 721–734.
- [41] E. Fermi, J. Pasta, and S. Ulam, Studies on nonlinear problems, I, Los Alamos Scientific Laboratory Report No. LA-1940 (1955). Reprinted in A.C. Newell ed., Nonlinear Wave Motion, AMS Lectures in Applied Math., Vol. 15 (1974) 143–156.